Science of the Total Environment 897 (2023) 165218

Contents lists available at ScienceDirect

Science of the Total Environment

journal homepage: www.elsevier.com/locate/scitotenv

New insights into the structure, microbial diversity and ecology of yellow biofilms in a Paleolithic rock art cave (Pindal Cave, Asturias, Spain)

Tamara Martin-Pozas [a], Angel Fernandez-Cortes [b,*], Soledad Cuezva [c], Juan Carlos Cañaveras [d], David Benavente [d], Elsa Duarte [e], Cesareo Saiz-Jimenez [f], Sergio Sanchez-Moral [a]

[a] Department of Geology, National Museum of Natural Sciences (MNCN-CSIC), 28006 Madrid, Spain
[b] Department of Biology and Geology, University of Almeria, 04120 Almeria, Spain
[c] Department of Geology, Geography and Environment, University of Alcala, Campus Cientifico-Tecnologico, 28802 Alcala de Henares, Spain
[d] Department of Environmental and Earth Sciences, University of Alicante, Campus San Vicente del Raspeig, 03690 Alicante, Spain
[e] Department of History, University of Oviedo, 33011 Oviedo, Spain
[f] Department of Agrochemistry, Environmental Microbiology and Soil and Water Protection, Institute of Natural Resources and Agricultural Biology (IRNAS-CSIC), 41012 Seville, Spain

HIGHLIGHTS

- Yellow biofilms threat Pindal Cave paintings.
- Classification by color is not enough to describe cave biofilms.
- Proliferation of yellow biofilms is associated to vapor condensation processes.
- Bacterial major genera in yellow biofilms were *Crossiella*, wb1-P19, *Nitrospira* and *Arenimonas*.
- *Actinomycetota* are the primary colonizers forming the branches of yellow biofilms.

GRAPHICAL ABSTRACT

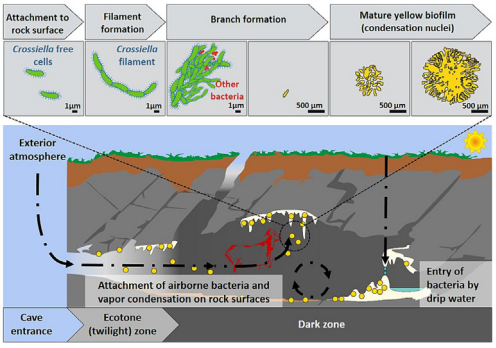

ARTICLE INFO

Guest Editor: Xiaobo Liu

Keywords:
Yellow biofilm
Bioclimatic conditions
Microbial ecology
Crossiella
Nitrospira

ABSTRACT

In the absence of sunlight, caves harbor a great diversity of microbial colonies to extensive biofilms with different sizes and colors visible to the naked eye. One of the most widespread and visible types of biofilm are those with yellow hues that can constitute a serious problem for the conservation of cultural heritage in many caves, such as Pindal Cave (Asturias, Spain). This cave, declared a World Heritage Site by UNESCO for its Paleolithic parietal art, shows a high degree of development of yellow biofilms that represents a real threat to the conservation of painted and engraved figures. This study aims to: 1) identify the microbial structures and the most characteristic taxa composing the yellow biofilms, 2) seek the linked microbiome reservoir primarily contributing to their growth; 3) seed light on the driving vectors that contribute to their formation and determine the subsequent proliferation and spatial distribution. To achieve this goal, we used amplicon-based massive sequencing, in combination with other techniques such as microscopy, in situ hybridization and environmental monitoring, to compare the microbial communities of yellow biofilms with those of drip waters, cave sediments and exterior soil. The results revealed microbial structures related to the phylum *Actinomycetota* and the most characteristic bacteria in yellow biofilms, represented by the genera wb1-P19, *Crossiella*, *Nitrospira*, and *Arenimonas*. Our findings suggest that sediments serve as potential reservoirs and colonization sites for these bacteria

* Corresponding author.
E-mail addresses: tmpozas@mncn.csic.es (T. Martin-Pozas), acortes@ual.es (A. Fernandez-Cortes), soledad.cuezva@uah.es (S. Cuezva), jc.canaveras@ua.es (J.C. Cañaveras), david.benavente@ua.es (D. Benavente), duarteelsa@uniovi.es (E. Duarte), saiz@irnase.csic.es (C. Saiz-Jimenez), ssmilk@mncn.csic.es (S. Sanchez-Moral).

http://dx.doi.org/10.1016/j.scitotenv.2023.165218
Received 3 February 2023; Received in revised form 13 June 2023; Accepted 28 June 2023
Available online 6 July 2023

that can develop into biofilms under favorable environmental and substrate conditions, with a particular affinity for speleothems and rugged-surfaced rocks found in condensation-prone areas. This study presents an exhaustive study of microbial communities of yellow biofilms in a cave, which could be used as a procedure for the identification of similar biofilms in other caves and to design effective conservation strategies in caves with valuable cultural heritage.

1. Introduction

Cave paintings often show deterioration caused by natural processes in which microorganisms are significantly involved (Schabereiter-Gurtner et al., 2002a, 2002b; Bastian et al., 2010; Urzì et al., 2010; Saiz-Jimenez et al., 2011, 2012; Zerboni et al., 2022). The international community has recently recognized the need to protect and safeguard the world's cultural and natural heritage (https://unstats.un.org/sdgs/metadata/files/Metadata-11-04-01.pdf) in which cave rock art is included.

Caves represent unique habitats for the development of microbial communities due to particular environmental conditions and harbor a wide variety of microorganisms that inhabit water, sediments and rocks. It is common to find visible evidence of the activity of microorganisms in subterranean environments, covering walls, ceilings, sediments and speleothems. In fact, abundant individual colonies spread all over the rock surface and extensive biofilms are distinctly visible to the naked eye.

The biofilms show differences, especially in their size and coloration, from shades such as pink, gray to yellow or white (Cañaveras et al., 2001; Northup et al., 2011). They occur both in the form of small millimetric colonies, as well as large biofilms or microbial mats, and constitute the main threat of biodeterioration in Paleolithic cave paintings such as Tito Bustillo, Altamira and Lascaux caves, among others (Schabereiter-Gurtner et al., 2002a, 2002b; Bastian et al., 2010; Saiz-Jimenez et al., 2011). Although, the source of these biofilms in caves remains unclear, previous studies attempted to explain the origin and composition of cave microbial communities (Porca et al., 2012; Mulec et al., 2015; Riquelme et al., 2015a; Lavoie et al., 2017). From all the biofilms coating cave walls and ceilings, either in karstic or volcanic areas, one of the most outstanding and conspicuous are the yellow ones, widely distributed across the globe (Northup et al., 2011; Hathaway et al., 2014; Riquelme et al., 2015a, 2015b; Spilde et al., 2016; Kim et al., 2019; Selensky et al., 2021). However, most of these studies have not found a differential composition between colored biofilms and suggest that they are complex consortia composed of bacteria from the phyla *Actinomycetota*, *Pseudomonadota* (synonym *Proteobacteria* according to Oren and Garrity, 2021), *Acidobacteriota*, *Nitrospirota*, *Bacillota* (formerly known as *Firmicutes*), *Bacteroidota* and *Chloroflexota*, with a similar morphology.

Regarding karstic caves, Mulec et al. (2015) isolated different species of the genera *Bacillus*, *Flavobacterium*, *Paenibacillus*, *Pseudomonas*, *Staphylococcus*, *Streptomyces* and *Variovorax* from yellow biofilms in three Slovenian karstic caves. Porca et al. (2012) performed a comparative analysis of yellow biofilms growing on the walls of caves from Spain, Czech Republic and Slovenia, concluding that yellow biofilms share morphologically similar bacteria and were composed of phylotypes affiliated with the actinomycetotal suborder *Pseudonocardinae* and the gammaproteobacterial order *Chromatiales*. These authors also suggested that yellow biofilm colonization of caves occurs through water infiltration. Other authors suggested different pathways for long-distance microbial dispersion in caves, including airborne transport and transmission through biological vectors. Certain microorganisms enter caves from the external surface, while others become airborne through water splashing or the movement of sediment particles by animals or humans in the underground environment (Fernandez-Cortes et al., 2011; Mulec et al., 2017; Alonso et al., 2023).

Regarding volcanic caves, Lavoie et al. (2017) compared the cave distinct colored biofilm communities with the overlaying surface soil communities concluding that both communities differs substantially and cave communities are not a subset of surface soils. Riquelme et al. (2015b) characterized colored (yellow, tan and white) microbial mats in 13 volcanic caves from Azores Islands and reported that all the three colored biofilms contained some similar morphologies including filaments covered with hair-like and knobby extensions as well as beads-on-a-string. *Pseudomonadota*, *Actinomycetota*, *Acidobacteriota*, *Nitrospirota* and *Chloroflexota* were recovered from all caves and represented the majority of the phyla. Gonzalez-Pimentel et al. (2018) investigated the microbial diversity of yellow colored biofilms coating the walls of a volcanic cave in La Palma Island. RNA-based study showed that members of the phylum *Actinomycetota*, with 55 % of the clones belonging to the order *Euzebyales*, were metabolically active components.

The colonization and growth of microorganisms on cave paintings are complex processes, whose development is controlled by the interrelationship between different factors. Active biodeterioration processes in caves are closely related to significant biogeochemical cycles (Cuezva et al., 2012; Martin-Pozas et al., 2020, 2022a). Effective control strategies for their sustainable conservation require an in-depth understanding of the deterioration processes involved (Zerboni et al., 2022). It is necessary to know the substrata characteristics, but also the microbiome diversity, dispersal mechanisms, metabolic activity, etc. (Saiz-Jimenez et al., 2012; Porca et al., 2012; Sterflinger et al., 2018) and the characteristics of the surrounding heterogeneous environment (Laiz et al., 1999; Cuezva et al., 2009; Zhang et al., 2019; Ma et al., 2023).

In this work, we investigated the composition and structure of the microbial communities that constitute the yellow biofilms in Pindal Cave (Asturias, northern Spain). This cave, as part of Paleolithic cave art of northern Spain, is an UNESCO World Cultural Heritage Site (https://whc.unesco.org/en/list/). The development of yellow biofilms in Pindal Cave constitutes a real threat to the conservation of the wall paintings. The objective of the work is to identify the populations that constitute the yellow biofilms, characterize their structure, determine their distribution patterns based on the different substrates and environmental conditions of the cave, and identify the possible microbial reservoirs that contribute to their formation and subsequent proliferation. We hypothesize that microbial communities of caves come from the surface and are molded in subsurface environments by environmental factors and the characteristics of each substratum. In order to clarify the origin of these biofilms, a characterization of the exterior soils, cave sediments and cave drip waters has been carried out, by means of an extensive characterization combining molecular techniques of fluorescent in situ hybridization (FISH), metabarcoding, electron microscopy and environmental monitoring. A comprehensive understanding of the indicator microbial groups, the origin and the factors that favor the development of yellow biofilms is essential to design adequate and sustainable conservation strategies in these underground environments that house valuable cultural heritage.

2. Materials and methods

2.1. Site description and sampling

Pindal Cave (Asturias, Spain) is a limestone cave, open to the public with limited guided tours. Since 2008, Pindal Cave was inscribed as UNESCO World Heritage because of its Magdalenian and pre-Magdalenian paintings (González-Pumariega Solís, 2011). The cave has a single wide entrance at 24 m above sea level, near the coastline. Jimenez-Sanchez et al. (2006) previously described the cave geomorphology. The main panel, with profusion of engravings and paintings, is around 250 m from the entrance. In general, the paintings show a good state of conservation, but in recent times the development of yellow biofilms has been

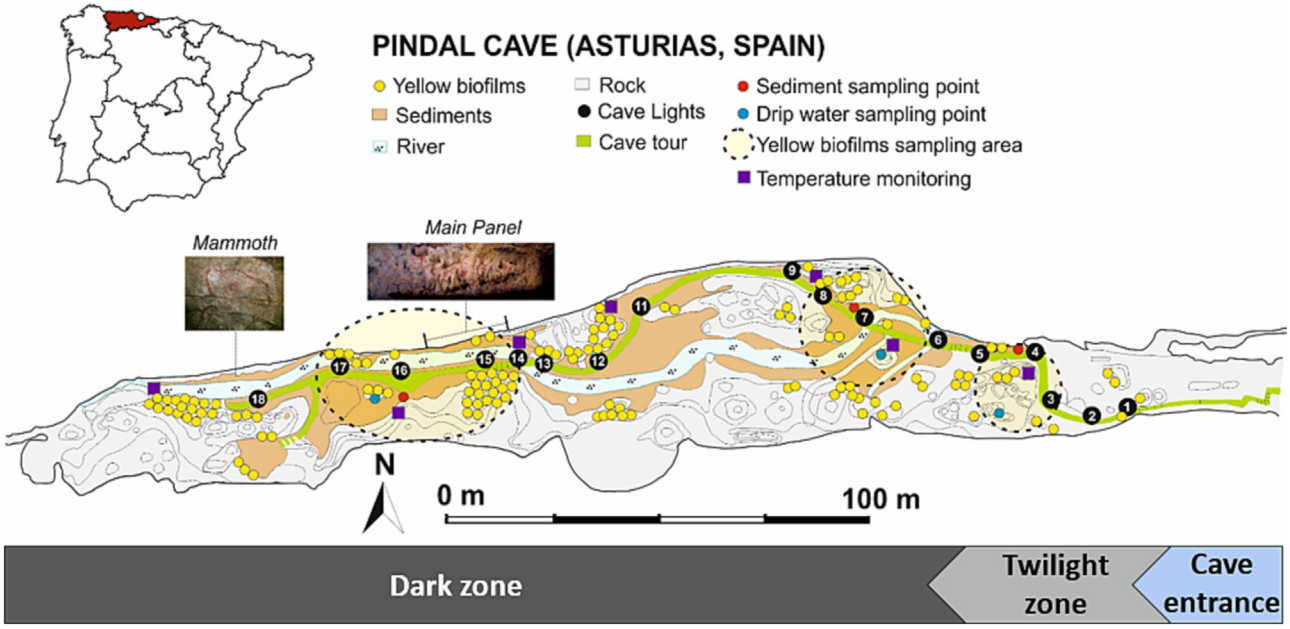

Fig. 1. Spatial distribution of yellow biofilms, sediments, and sampling location in Pindal Cave.

observed in some localized areas and very close to the paintings on the main panel.

Fig. 1 shows the topography of the touristic sector of Pindal Cave with the spatial distribution of sediments, drip waters and yellow biofilms. For the definition of the sampling areas within the cave, the lighting points (sites) of the touristic route have been used (numbered from 1 to 18). All samples were collected during several fieldwork campaigns during the environmental monitoring period. The sampling sites were selected trying to cover the entire mapped cavity, including the main panel with paintings, which highlights an extensive development of yellow biofilms (Fig. 5j–n). To understand the origin of the biofilms and their relationship with sediments and drip waters, this study compare the bacterial communities of the exterior soil, with the sediments, drip waters and yellow biofilms of twilight and dark zones inside the cave. Two biological replicates of the forest soil samples at a depth of <10 cm overlaying the site 4 and two biological replicates of cave sediment samples at a depth of <10 cm, for each sampling location, were sequenced. These locations comprise the i) ecotone or twilight zone, close to the natural entrance of the cave in site 4, ii) central gallery, located in the middle zone, in site 7, and iii) final gallery, located at the end, in site 16. The water drips are not always active or provide very little amount of water along the time. Therefore, to obtain enough sample amount to geochemical characterization and sequencing, we performed three fieldwork campaigns to collect eight drip water samples in the nearest locations to cave sediment-sampling point: three samples from site 3, two site 7 and three site 16. For yellow biofilms, the sampling strategy to obtain enough sample amount was sample pooling. Five yellow biofilm samples for sequencing were collected from the walls and speleothems at the previously mentioned sites. One biofilm sample was collected at site 4, another at site 7, and three samples at site 16. Among these three samples, two were specifically obtained from the painting panel (Fig. 1 and Table S1). To ensure the consistency of yellow biofilms, we sampled individual yellow biofilms and verified their yellow shade and structure under the microscope.

2.2. Physicochemical properties of cave sediments

Mineralogical analysis of the ground sediment samples was carried out in a Bruker D8 Discover A25 microdiffractometer. The chemical characterization of sediments was carried out using the methods described by Martin-Pozas et al. (2022a). The particle size distribution was determined using a column of mesh sieves between 2 mm to 0.063 mm of light and the silt-clay fraction using a Coulter LS230 laser granulometer (Walker and Hutka, 1971). The statistical analysis of the data was performed with the statistics package Gradistat (Blott and Pye, 2001).

2.3. Physicochemical properties of the drip water

The chemical composition of groundwater was determined by ion chromatography (DIONEX DX 500) and by inductively coupled plasma mass spectrometry, ICP-MS (VG PQ-ExCell, THERMO ELEMENTAL). Bicarbonates were measured through neutralization titration. Temperature and pH were measured in situ with a portable multiparameter HI9829 (HANNA Instruments).

ATP concentration in drip waters was used as a measure of biomass and microbial activity. ATP was quantified by bioluminescence analysis using a PhotonMaster™ luminometer (PhotonMaster EQP-PMT) and LuminUltra Water QGA test kit, strictly following the instructions manufacturer.

The saturation state of calcite and equilibrium CO_2 partial pressure (pCO_2) was performed using PHREEQC code using 3.4.0 version (Parkhurst and Appelo, 2013).

2.4. Environmental monitoring

Cave air temperature was recorded every half-hour for an entire hydrological year (October 2021–September 2022) by using a network of seven Tinytag TGP-4500 dataloggers (Gemini, UK) each one equipped with a thermistor sensor with an accuracy of ±0.5 °C between 0 and 40 °C and resolution of 0.01 °C. These devices were distributed along a transect from the entrance of the cave to the areas farthest from the exterior (Fig. 1), taking as a criterion the representation of the different changes in the section and directions of the galleries and using the cave lighting points for geo-reference. Measurements were taken at a height of 1 m from the cave floor. The Tinytag TGP-4500 dataloggers used in this study to measure relative humidity (RH) consist of in-built capacitive sensor (RH) that operates between 0 % and 100 % RH with an accuracy of ±2 % from 0 to 90 % and ±3 % from 90 to 100 %. These devices allow obtaining RH averages with a resolution of 0.01 %, which facilitates the detection of small humidity changes in non-saturated conditions. However, the time-response of this capacitive sensor is too long to detect short or medium-term variations of RH under prevailing cave conditions of vapor-saturation, except for those areas

closest to the cave entrance where some masses of colder and drier air from outside occasionally enters the cave. Accordingly, the RH data were not considered in the spatiotemporal analysis of cave microclimate.

2.5. Low resolution optical microscopy

Detailed pictures of yellow colonies were taken in situ with a digital microscope Dino-Lite (model Edge AM4115ZT) and in the laboratory with a Leica M165C stereoscopic microscope. In the last case, once collected samples in the cave, were kept at 4 °C and observed in a time not exceeding 48 h.

2.6. Electron microscopy

Textural and ultrastructural characterization of different yellow colonies was performed by environmental scanning (ESEM) and transmission electron microscopy (TEM).

For ESEM, samples were stored in a silica-gel desiccator, at least two days, to eliminate excess moisture and avoid lose the structure of the colonies. Then, to improve the quality of the photographs the samples were coated with gold and observed under high vacuum conditions, at 20–30 kV accelerating voltage under an ESEM Inspect (FEI, USA).

Samples for TEM were fixed using 4 % formaldehyde and 2 % of glutaraldehyde in 0.1 M PBS and pH 7.4 and embedded in gelatin at 15 %, followed by chemical post-fixation using osmium tetroxide and uranyl acetate and exposed to an ethanol dehydration series of 50, 70, 90 and 3 × 100 % (v/v). Once dehydration is complete, the samples were embedded in LR-White methacrylate resin and polymerization was carried out at 60 °C for 48 h. The ultrathin sections were sliced on an ultramicrotome. Then, the sections applied onto grids coated with Formvar film, and contrasted with lead citrate and uranyl acetate were mounted on microscope grids, and observed in a Transmission Electron Microscope JEM1400 Flash (Jeol, Japan) at 100 kV accelerating voltage.

2.7. Confocal microscopy and CARD-FISH

Confocal microscopy combined with the Fluorescent in Situ Hybridization (FISH) technique was used to complement the structural information obtained from electron microscopy and compositional metabarcoding analyses. In this work, we used the CARD-FISH technique to obtain a more intense signal (Hoshino et al., 2008).

CARD-FISH experiments were performed on filters following the protocol described in detail by Pernthaler and Pernthaler (2007) with minor modifications. Colonies samples were fixed in situ with 4 % formaldehyde for 2 h at 4 °C and stored in phosphate buffer PBS (NaCl 8 g/l, KCl 0.2 g/l, Na_2HPO_4 1.44 g/l, KH_2PO_4 0.24 g/l) 0.1 M pH 7.4 at −20 °C until further processing. For cell wall permeabilization, filters were treated with lysozyme and achromopeptidase solutions. Endogenous peroxidases were inactivated using 0.15 % H_2O_2 in methanol as described in Ishii et al. (2004). Probes for the most abundant bacterial taxa were used: i) GAM42a and GAM42a_T1038 specific for the class *Gammaproteobacteria* and ii) HGC236 specific for the phylum *Actinomycetota*. Hybridization was performed with 5′-HRP-labeled oligonucleotide probes (Biomers, Germany) for 2 h at 46 °C and then filters were washed at 48 °C for 10 min. Tyramide signal amplification was carried out for 45 min at 46 °C. Formamide (FA) and NaCl concentration for each probe in hybridization and washing buffer used are summarized in Table S2. Filters were counterstained with propidium iodide (Thermo Fisher Scientific, USA), according to manufacturer instructions, covered with the Vectashield: Citifluor mixture, mounted in glass slides and looked at under a microscope. The samples were photographed with a Zeiss LSM 780 high-resolution confocal microscope with Airyscan.

Previous studies suggested that yellow biofilms are formed mostly by bacteria and not by eukaryotic organisms (Porca et al., 2012; Riquelme et al., 2015a, 2015b; Lavoie et al., 2017; Gonzalez-Pimentel et al., 2018). Therefore to assess the presence of fungi within the yellow biofilms, we applied a combination of specific probes for the most common phyla (FAsc_1094 specific for the phylum *Ascomycota* and FBas_757 specific for the phylum *Basidiomycota*) with CalcoFluor White (Sigma- Aldrich) staining, as described in Priest et al. (2021). The stain CalcoFluor White is a non-specific fluorescent dye that binds to chitin and cellulose. Then the results were analyzed in a confocal laser scanning microscope (Zeiss ELYRA LSM780).

2.8. DNA extraction, bacterial 16S rRNA metabarcoding

Genomic DNA from sediments and external soils was extracted using DNeasy Powersoil DNA extraction kit (Qiagen, Germany). For the colonies and drip waters, the extraction kits used were DNeasy PowerBiofilm and DNeasy PowerWater (Qiagen, Germany). The library preparation was carried as detailed by Martin-Pozas et al. (2020). The primers used to study the population of bacteria were Bakt 341F and Bakt 805R (Herlemann et al., 2011). To assess the presence of fungi within the yellow biofilms, the primer pairs of ITS86F and ITS4 were used (White et al., 1990). We included negative controls without DNA to control the contamination during the extraction of genetic material, as well as negative controls to control contamination during library preparation. The set of the libraries were sequenced at the facilities of the company AllGenetics & Biology S.L (A Coruña, Spain) in an Illumina MiSeq platform (PE300).

The analysis of the readings provided by the service of sequencing was performed using bioinformatics software QIIME II (Bolyen et al., 2019) and DADA2 (Callahan et al., 2016). Taxonomic assignments were performed by querying the sequence reads against the SILVA SSU 138 reference database (Quast et al., 2013). Sequences identified as *Archaea* (with relative abundances below 1 %), chloroplast, and mitochondria were removed. Afterwards, the ASV table was processed using the phyloseq library (McMurdie and Holmes, 2013) from RStudio (v3.6.0) and the results of abundance of ASVs are expressed in relative abundances. Alpha diversity was calculated using Shannon, Simpson diversity and Chao1 evenness indices and significance was determined using the Kruskal-Wallis test. Rarefaction curves were plotted using vegan function rarecurve of vegan package. Differences between samples, the beta diversity, was visualized with Bray Curtis dissimilarity and non-metric multidimensional scaling (NMDS) using the function metaMDS in the vegan package. The association of physicochemical data with the beta diversity summarized with the NMDS ordination was analyzed with the envfit function in vegan. In addition, differences in community composition between samples were tested by permutational analysis of variance (PERMANOVA) and the nonparametric analysis ANOSIM, with 999 permutations and Bray Curtis distance, using the vegan package in R.

Exclusive and shared ASVs between samples were detected using a Venn diagram. Spearman's correlation among the most abundant bacterial taxa (with ≥1 % read in at least one sample) was calculated using Hmisc and corrplot packages in R package. The correlation coefficients over 0.6 and P-value bellow 0.05 of the most abundant taxa were imported and visualized as co-occurrence networks in Cytoscape software.

3. Results

3.1. Physicochemical properties of the sediments and other cave deposits

The results of the textural, geochemical and mineralogical analyses of the sediments are shown in Table S3. Gravity coarse-grained deposits constituted of a mixture of small breakdown blocks of bedrock and speleothems with sands and clays are mainly found at site 4. On the other hand, sediments from sites 7 and 16 are water flow clastic fine-grained deposits (Fig. S4). According to their textural, chemical and mineralogical composition the cave sediments can be described as brown siliceous silty sands with moderate-high contents, and quartz predominates over calcite, vermiculite, illite and kaolinite. The sediments have relatively high organic matter contents and moderately basic pH (7.9–8.5). Geochemical analyses reveal differences between samples, especially with regard to the site 4

area, where parameters such as organic matter, nitrogen, ammonium, nitrate content, electrical conductivity and water content are remarkably lower than at the other points. The sediments at the cave entrance would be expected to be richer in carbon and organic matter. However, sandy textures have great porosity, which facilitates aeration and water circulation and, on the contrary, is not capable of retaining water or ionic nutrients, which would explain the lower content of nitrogen and organic matter.

3.2. Physicochemical properties of the drip water

The chemical analysis of the dripping waters shows moderate to high mineralization (Table S4). Consequently, dripping waters are saturated in calcite with a basic pH and high Ca^{2+} and HCO_3^- concentrations. These waters can be classified as HCO_3-Ca type, with SO_4^{2-} and Mg contents ranging from 1 to 5 %; Cl^- and Na^+ contents ranging from 10 to 21 % and from 8 to 15 % respectively. These relatively high values in Cl^- and Na^+ contents in the infiltration waters reflect the input of sea salts near the coast by means of aerosol effect. Marine aerosols are accumulated on the soil over the cave and they are dissolved and introduced into the cave after rain events. Thus, D4 contains the highest marine ion concentrations because it is the point of infiltration closest to the coastline.

3.3. Environmental monitoring

The punctual and periodic measurement of air temperature in a network of sampling points allowed us to obtain different snapshots over time of the bioclimatic zoning of the subterranean environment to be correlated with the spatial distribution patterns of the cave microbial communities. The spatial maps of cave air temperature were constructed using geostatistical gridding based on an ordinary point kriging method with a linear variogram model. During interpolation, a preferential direction was considered for characterizing the spatial variability of cave air temperature as a function of distance from the cave entrance.

Fig. 2 summarizes the spatial distribution of both the annual mean of temperature and the mean daily range of air temperature at Pindal Cave, during the hydrological year 2021–2022. The morphology of the cave in its first 100 m, with its only entrance situated at a higher altitude and a stepwise downward slope, favors a negative temperature gradient as a function of distance to the exterior and a prevailing entrapment of a cold air mass throughout the year (temperature lower than 11.8 °C, on average values). This air mass extends to the intermediate zone of the cave (site 9) and is clearly influenced by the meteorological fluctuations outside and by a greater aerodynamic mixing with the local atmosphere. Thus, this cave sector registers notable daily variations in temperature in a range between 0.15 and 0.35 °C/day, as well as a marked gradient in these daily variations.

The second sector of the cave, from site 9 towards the more distal area of the entrance, develops along an almost flat slope. In this sector, there is an accentuated positive thermal gradient as a function of distance to the exterior (from 11.80 to 12.15 °C) and a prevailing entrapment of a warmer air mass throughout the year, in contrast to the average thermal pattern of the first sector. In this second sector, the mean daily thermal variations are considerably attenuated (<0.15 °C/day) with a marked spatial homogenization.

The mean annual temperature outside the cave is 12.14 °C, very close to mean annual cave temperature recorded in the cave during the study period (11.91 °C). Within the hydrological cycle 2021–2022 (Fig. 3), the mean temperature of cave air varied throughout the year in a narrow range between 11.8 °C (February) and 12.63 °C (September), with a seasonal evolution similar to the outside temperature. A first thermal pattern can be distinguished from November to the beginning of May, in which the cave temperature is higher than the outside temperature (between 1.0 and 4.3 °C higher, taking into account the record in all locations). During winter period, the short-term variations in temperature are more intense, particularly in the locations closest to the entrance, which denotes the preferential entry of cold and drier, external air in favor of a density gradient. This

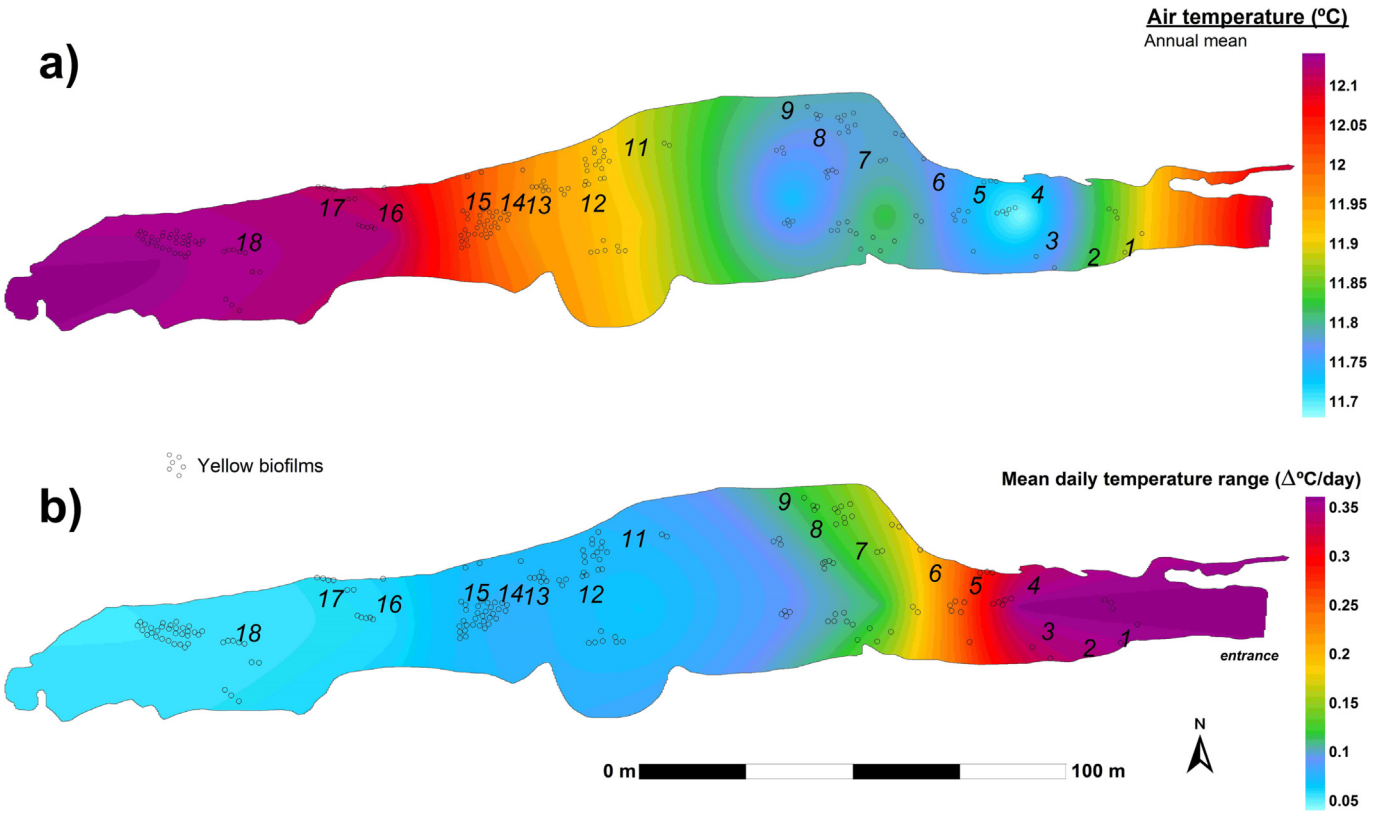

Fig. 2. Spatial distribution of the air temperature at Pindal Cave: a) annual mean and b) mean daily range. Monitoring period: October 2021–September 2022. The distribution of the yellow bacteria colonies is drawn for comparison. Numbers indicate the cave lighting points (sites) along the tourist path.

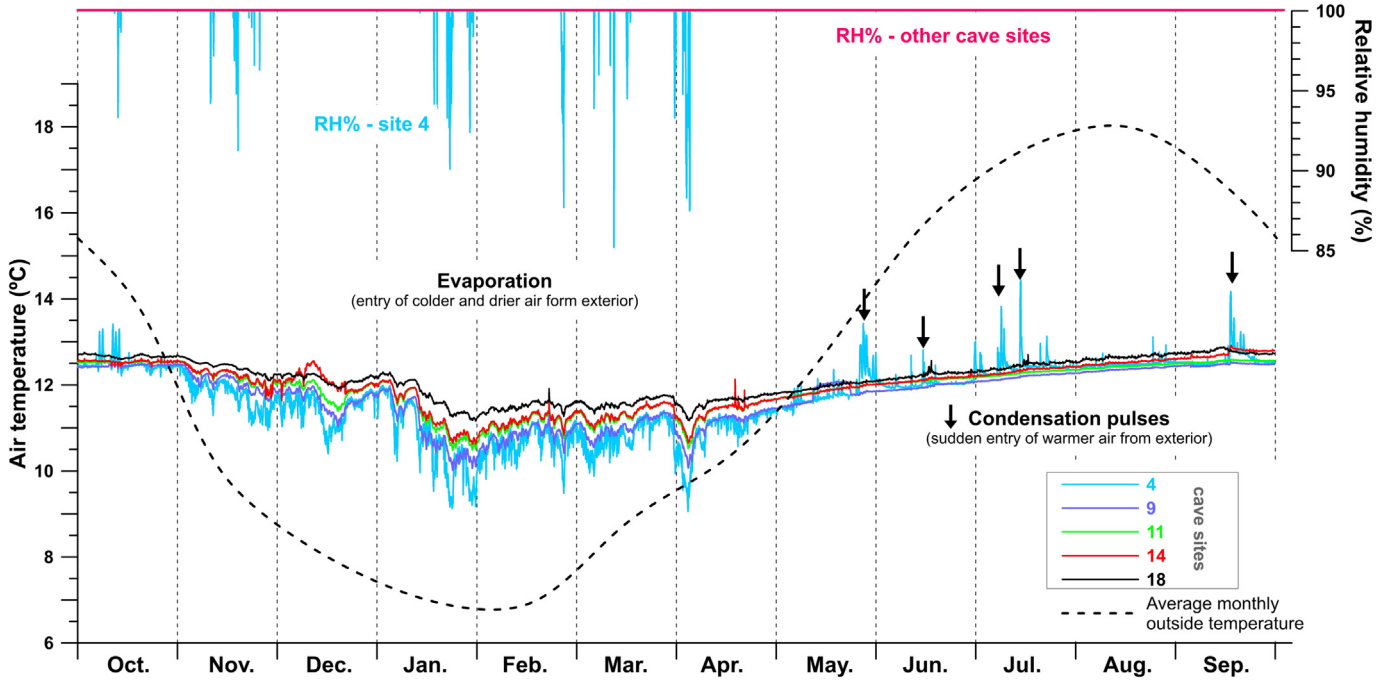

Fig. 3. Half-hourly series of air temperature and relative humidity at different cave locations compared to the average monthly temperature at exterior, during the monitoring period: October 2021 – September 2022. Monthly temperature data at exterior are based on the European Centre for Medium-Range Weather Forecasts data (ECMWF), considering the average for the years 1991–2021 (https://es.climate-data.org/) for Colombres village (2.5 km far from the cave).

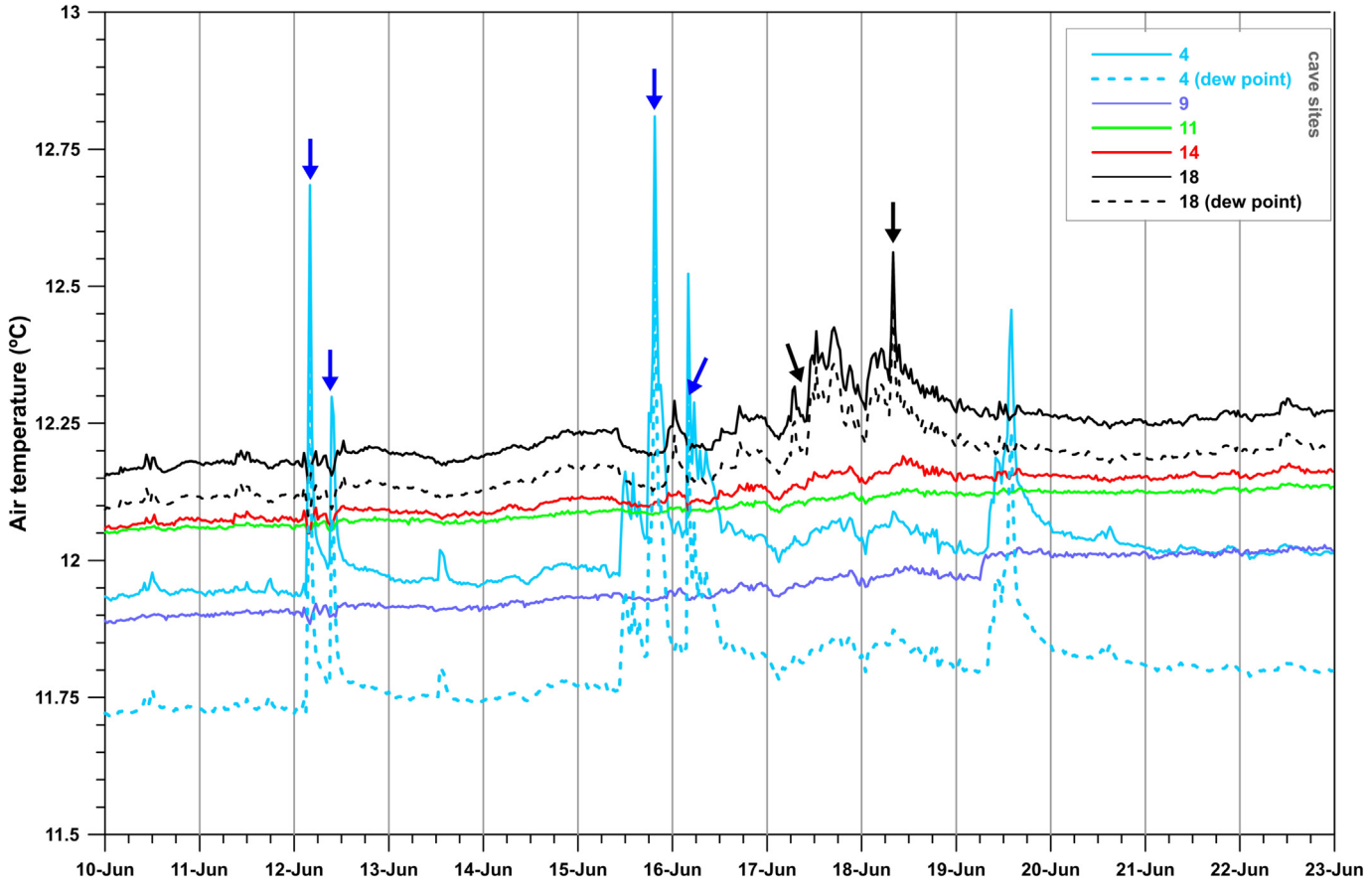

Fig. 4. Half-hourly series of air temperature (continuous lines) and dew point temperature (dashed lines) at different cave locations during the middle of June 2022. Sudden rises of air temperature in sites 4 and 18, which equalize with the dew point temperature, reveal the occurrence of condensation pulses (labeled with colored arrows).

causes the average temperature of the cave to drop approximately 1.5 °C (from 12.55 to 11.08 °C) and relative humidity decreases below 95 % for short periods of time (Fig. 3).

In contrast, from May to October, a second thermal pattern is distinguished with an average outside temperature progressively increasing above the average cave temperature, reaching a maximum difference of

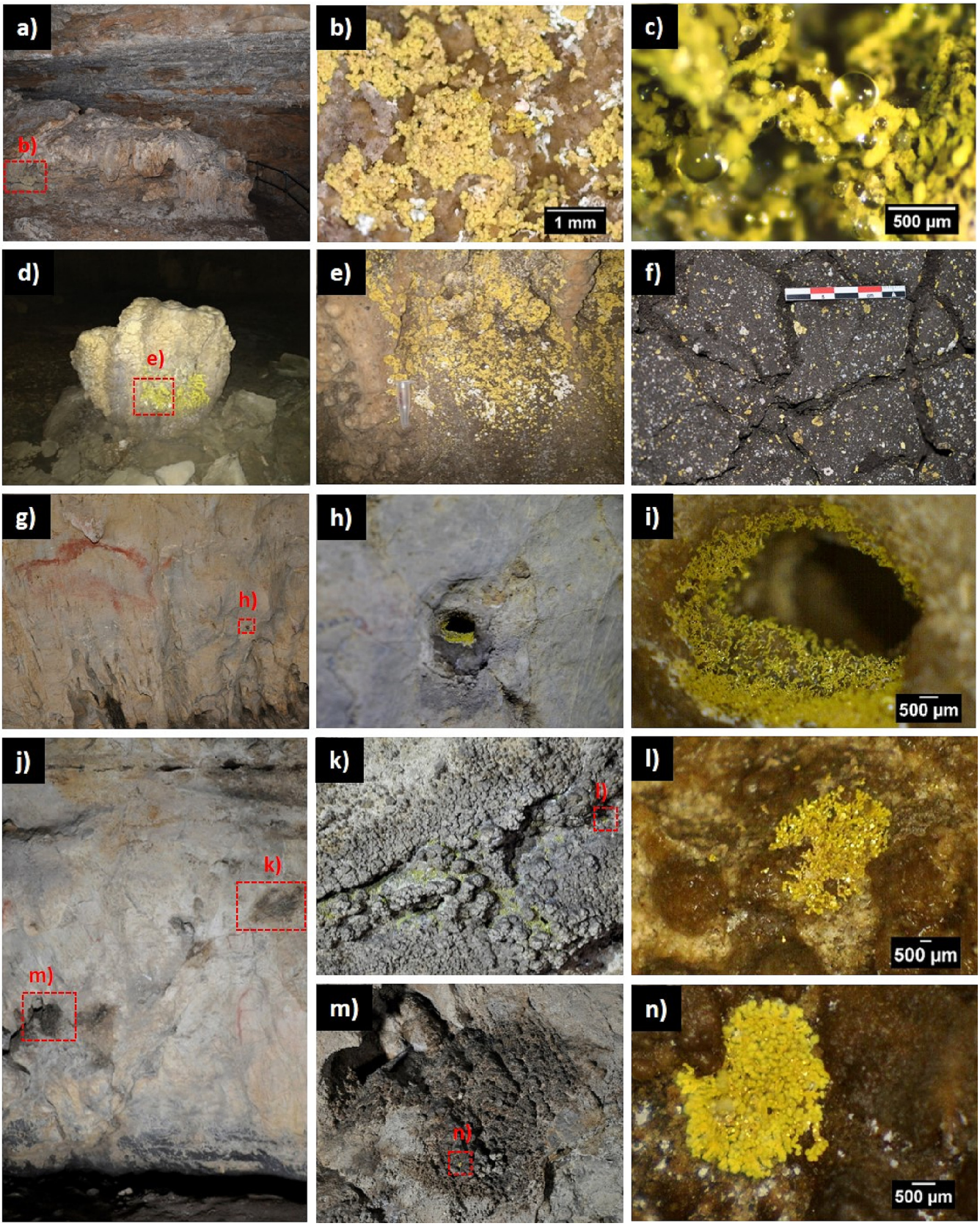

Fig. 5. Yellow biofilms description and location. a–c) Site 4 (near the cave entrance), d–f) site 7, g–n) site 16 (main panel).

5.5 °C in August. In this second period, the average cave temperature increases progressively from approximately 11.8 to 12.7 °C, and the thermal differences between cave zones are minimized. During the summer thermal pattern, short-term temperature variations are minimal throughout the cave, except for the entrance area (site 4) where sharp temperature rises of >0.5 °C are frequently recorded compared to the rest of the locations. These events are generated by the sudden entry of warmer outside air, causing intense condensation processes preferably on the rock and speleothem surfaces of this area of the cave. Consequently, the condensation of water vapor on the surfaces of rock and cave sediments is triggered once the cave air temperature equalizes with the dew point temperature (Fig. 4), considering these surfaces remain colder than cave air and under constant water saturation (relative humidity equal to 100 %). Although with less intensity (0.2–0.4 °C) and periodicity, these thermal pulses are also produced in the area furthest from the main entrance (Fig. 4). This phenomenon points to a direct connection with the outside in that area (site 18), which explains the presence of visible condensation surfaces in that area during the summer season. The condensation droplets persist over time and were observed during our different multipurpose sampling campaigns.

3.4. Microscopic characterization of yellow biofilms

The yellow biofilms are predominantly found on rough and hard surfaces throughout the eastern sector of the cave (Fig. 1). In situ observations indicate that these biofilms commonly develop on surfaces with rough textures that facilitate the accumulation of water due to surface tension (Fig. 5e, k, m). Examples of such surfaces include rough rock-speleothem surfaces (Fig. 5a, d, k, m) and within small voids (Fig. 5h–i). In some areas with high levels of condensation, yellow biofilms also proliferate on the surface of the sediments (Fig. 5f).

The color tone of yellow biofilms varies from lighter to darker shades depending on the location (Fig. 5). The dimensions and morphology of the biofilms also vary: from small ramifications <500 μm (Fig. 5i), isolated circular and filamentous biofilms of 2–5 mm (Fig. 5f, l, n), to irregular

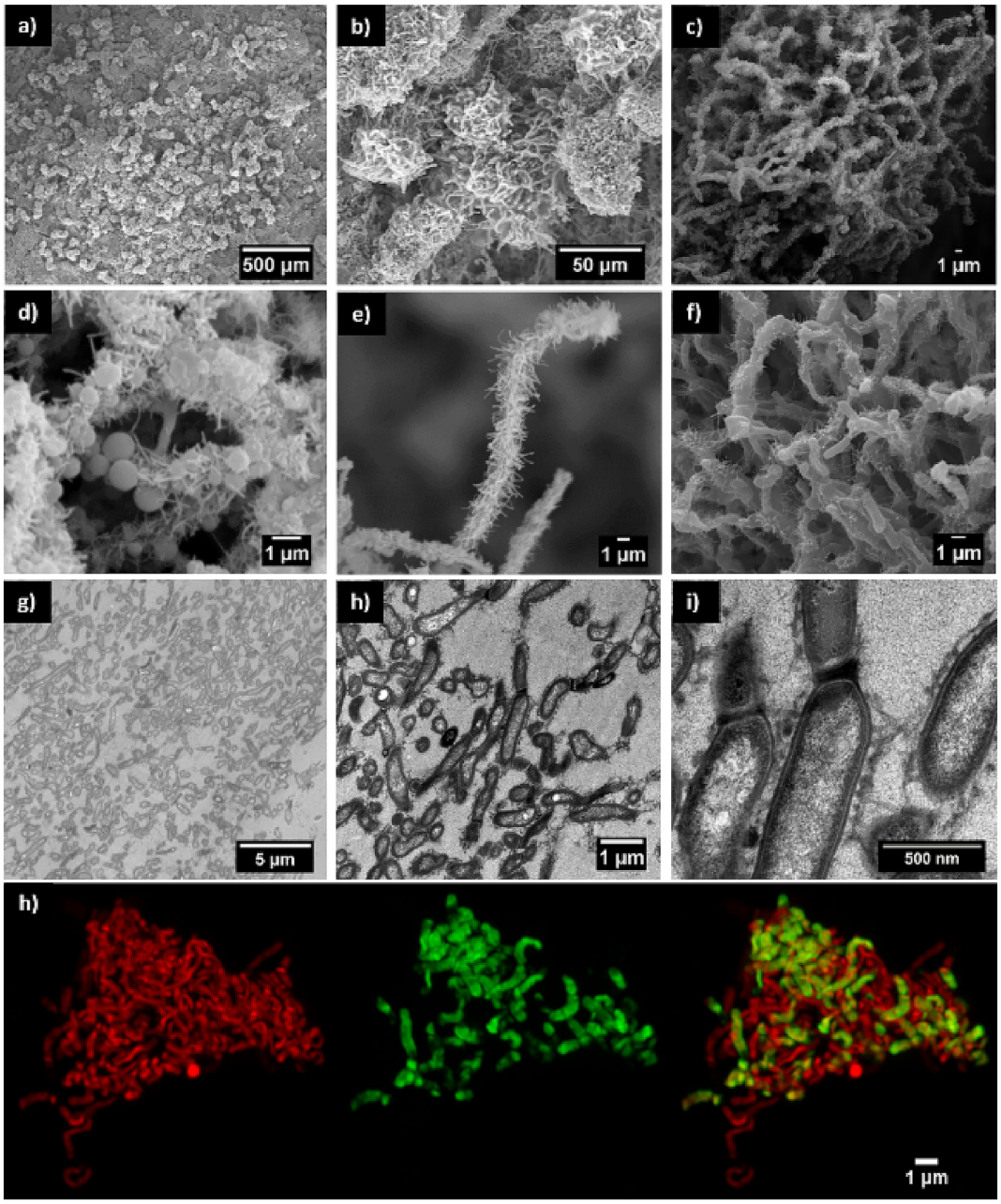

Fig. 6. Microscopy of yellow biofilms. a–f) SEM, g–i) TEM, h) Airyscan microscopy and CARD-FISH (*Actinomycetota* in green, DNA in red).

biofilms forming mats with an extension of several cm^2 (Fig. 5a–b). However, at the microscopic level the biofilms present a homogeneous structure. They are composed of small branches of about 20–70 μm, with a woolly appearance and retained water droplets on their surface (Figs. 5c, 6b). Branches are formed by a network of cocci-shaped cells of 0.5–1 μm and long filaments with fimbriae or protuberances (Fig. 6c–f), which are distributed along its surface, composed of bacillary cells 1.7 μm long and 0.4 μm wide (Fig. 6f–i).

The CARD-FISH technique showed a positive signal in the filaments composed of rods that form the branches when the *Actinomycetota*-specific probe HGC236 was used (Fig. 6h). Positive CARD-FISH signals were not obtained when GAM42a and GAM42a_T1038 were used, so they are probably not specific for the taxa present in the samples. Positive signals were not obtained when FAsc_1094, FBas_757 and CalcoFluor White were used, so fungi do not form the yellow biofilms. To our knowledge, CARD-FISH technique has not previously been used in cave studies, and therefore, our results cannot be compared with other caves. No positive signal was obtained with the probe in the cocci-shaped cells associated with the branches (Fig. 6h).

3.5. Microbial community diversity

Alpha diversity values for each substrata were determined at the genus level using Chao1, Shannon, and Simpson indices (Fig. 7a and Table S5). Alpha diversity analyses showed relatively high diversity indices in yellow biofilms, but no significant differences were observed between the samples (Kruskal-Wallis, P-value > 0.05).

The beta diversity estimates suggest that bacterial populations in the yellow biofilms were significantly different from the populations in the soils, sediments and drip waters (PERMANOVA and ANOSIM P < 0.05) (Table S6). Graphically, NMDS also showed significant differences between drip waters and the other substrata, meanwhile the populations in the sediments and the yellow biofilms were more similar (Fig. 7c). Collectively, these results suggest that water communities significantly differed from the others but biofilms communities were similar to sediments, especially to sediments in the site 4.

3.6. Taxonomic composition

In order to know the contribution of the surface ecosystem to Pindal Cave communities, this study compare the microbial communities from the exterior soil, drip waters, sediments, and yellow biofilms (Figs. 8, 9 and Table S7) from three different locations inside the cave (Fig. 1 and Table S1). The analyses of the reads obtained with the pair of fungal primers (ITS86F-ITS4) did not generated high quality sequences. Therefore, fungi were not present on the yellow biofilms. The analyses of the reads obtained with the pair of universal primers (341F-805R) generated 584,319 high quality sequences, grouped in 812 bacterial ASVs. These ASVs were classified into 46 bacterial phyla, of which the most abundant sequences were associated with *Pseudomonadota*, *Verrucomicrobiota*, *Patescibacteria*, *Acidobacteriota*, *Actinomycetota*, *Planctomycetota*, *Bacteroidota*, *Chloroflexota*, and *Dependentiae* (Fig. 8). Among them, 168 ASVs were exclusive of drip waters and 98 ASVs were shared between all samples, representing 21 % and 12 % of the total sequences, respectively (Fig. 6b). The Venn diagram showed that biofilms and sediments shared 55 ASVs, representing 7 % of the identified ASVs. However, the largest overlap between sediments, biofilms and waters represented 16 % of the total ASVs, which suggest the importance of drip water for the development of cave microbial communities.

At the phylum level, *Pseudomonadota*, *Acidobacteriota*, *Actinomycetota*, and *Planctomycetota* represented >75 % of the total sequences in the yellow

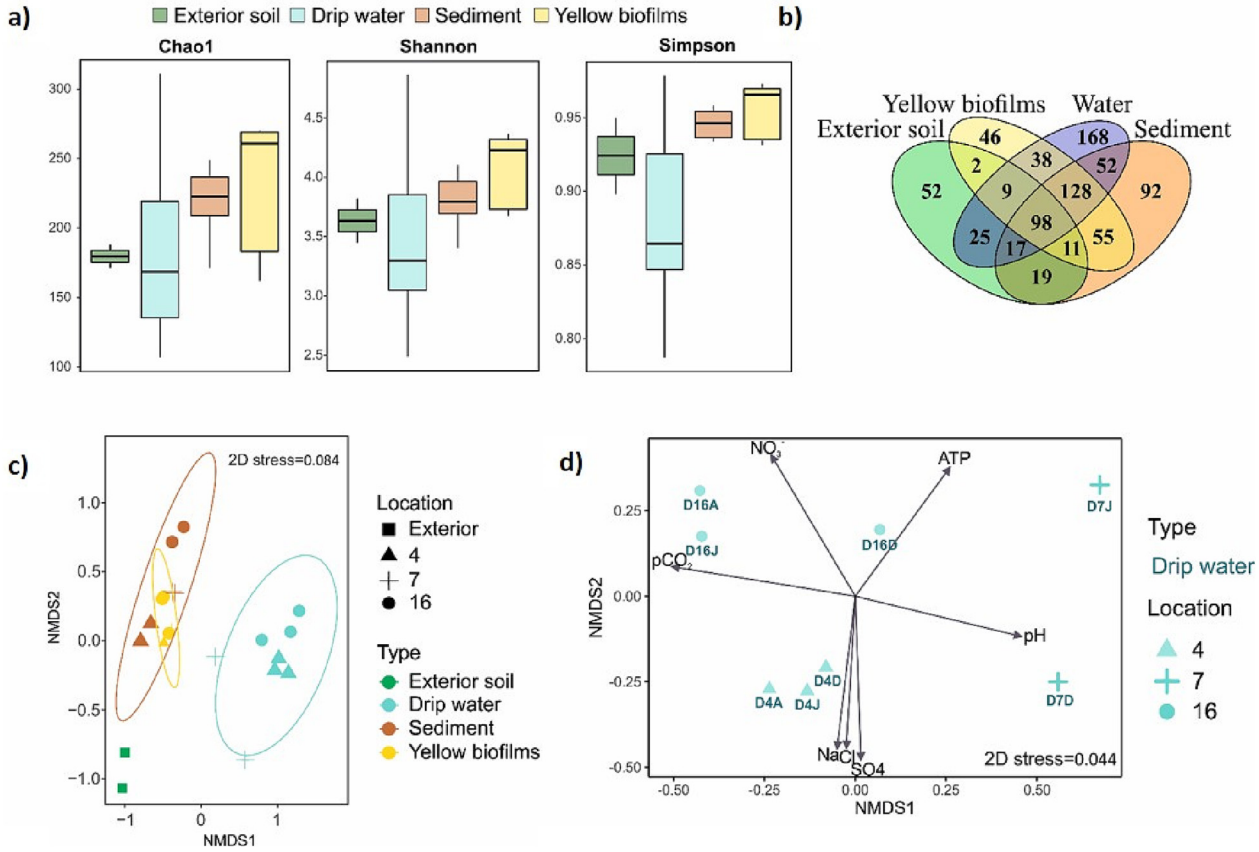

Fig. 7. Diversity analysis. a) Alfa Diversity indices: Composite evenness (Chao1) and diversity index (Shannon and Simpson) values from each sample type. b) Venn diagram showing the unique and shared ASVs between samples. c) NMDS plot showing Bray Curtis similarity between bacterial community compositions at the genus level for all sample type. Ellipses represent where 95 % of the data fall. d) NMDS analysis with physicochemical parameters of drip water samples.

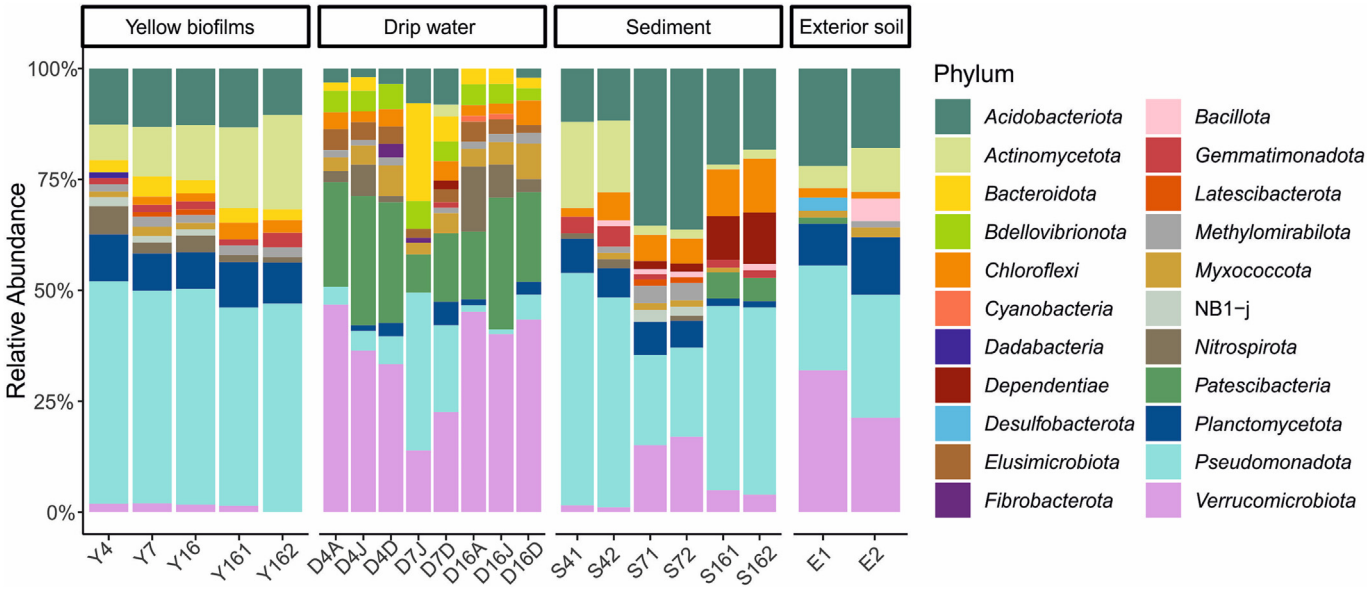

Fig. 8. Barplot shows the relative abundances reads classified at the phylum level in each sample. Phylum with relative abundances lower than 1 % are not shown.

biofilms. In the sediments *Pseudomonadota*, *Acidobacteriota*, and *Actinomycetota*, accounted for 53.3–80.3 % of the total. In the drip waters, *Verrucomicrobiota*, *Patescibacteria* and *Pseudomonadota* reached 54.1–72.7 %, while in the exterior soil *Pseudomonadota*, *Verrucomicrobiota*, *Acidobacteriota*, *Actinomycetota* and *Planctomycetota* amounted over 85 % of the total sequences. Clear differences in phyla, depending of the sample types, were observed among yellow biofilms, sediments, drip waters and exterior soils. Generally, biofilms and sediments presented high percentages of *Acidobacteriota* and *Pseudomonadota*, while *Patescibacteria* and *Verrucomicrobiota* dominated drip waters (Fig. 8). Among drip waters, great differences were observed depending on the location (Fig. 7d). In site 7, the abundance of the phylum *Pseudomonadota* was higher (18.5–33.5 %) than in other locations (1.0–6.1 %), which indicate a different karstic way than the rest of the drip waters in the cave.

At the genus level (Fig. 9), the yellow biofilms were characterized by the abundance of wb1-P19 (*Nitrosococcaceae*), followed by *Crossiella* (*Pseudonocardiaceae*) and *Nitrospira* (*Nitrospiraceae*). Relative abundances ranging between 1 and 5 % in Pindal yellow biofilms were assigned to unknown *Vicinamibacteraceae* (*Acidobacteriota*), the gammaproteobacterial group PLTA13, and the genera *Steroidobacter* and *Arenimonas*.

The sediment samples were also characterized by the abundances (>10 %) of the genera wb1-P19 and *Crossiella* in at least one of the samples, but uncultured *Vicinamibacterales*, TRA3-20, *Aquicella*, Ga0074140 and unassigned *Babeliales* also showed relative abundances above 10 % (Fig. 9). The genera wb1-P19 and *Crossiella* only appeared with abundances above 5 % in the site 4. Other bacteria worth of mentioning in Pindal sediments were *Sphingomonas*, uncultured *Anaerolineaceae*, Ga0077536 and uncultured *Gammaproteobacteria*, with relative abundances above 5 %.

The microbial communities of Pindal drip waters showed a completely distinct structure with phyla mostly absent in the biofilms and sediments, and abundances of prokaryotic *Candidatus* taxa contrasting with other Pindal samples (Fig. 9). The most abundant genus is by far *Candidatus* Omnitrophus (5.3–42.3 %) followed by the *Leptospirillum* (0.16–14.2 %), env.OPS 17 (0–9.6 %), *Candidatus* Nomurabacteria (0.03–9.26 %), *Candidatus* Kerfeldbacteria (0.3–8.0 %), *Candidatus* Yanofskybacteria (0.2–5.3 %), *Candidatus* Portnoybacteria (0–3.5 %), and *Candidatus* Azambacteria (0–2.8 %), *Vicinamibacteraceae* (0–2.8 %), and *Parcubacteria* (0.1–2.5 %). Other minor lineages with relative abundances ranging from 0.1 to 5 % in Pindal drip waters were SAR202 clade, bacteriap25 and 0319-6G20.

In the exterior soil samples, the high relative abundance of *Candidatus* Udaeobacter (17.7–28.7 %) was remarkable. Second in abundance (4.3–9.4 %) appeared the subdivision 2 of *Acidobacteriota* followed by other bacteria with relative abundances >3 %: uncultured *Gemmataceae*, uncultured *Elsterales*, uncultured *Acidobacteriales*, *Streptomyces*, unassigned *Xanthobacteraceae*, and *Reyranella* (Fig. 9).

4. Discussion

4.1. Common morphological aspects and core of bacteria in yellow biofilms

Yellow biofilms are the most studied microbial mats, since they are abundant and easy to distinguish. Thus, we find references to yellow biofilms with a similar morphology to Pindal in lava and limestone caves across the world (Cuezva et al., 2009; Spilde et al., 2016; Riquelme et al., 2015a; Lavoie et al., 2017). No mineral precipitation associated with this type of biofilms has been observed in the samples studied; neither in the literature was found references to the presence of precipitates associated with yellow biofilms (Cuezva et al., 2009). There are more references on studies of yellow biofilms in caves around the world but they cannot be compared with those of this study, from a morphological point of view, since a microscopic study was not carried out (Porca et al., 2012; Hathaway et al., 2014; Kim et al., 2019; Selensky et al., 2021).

Although yellow biofilms from Pindal Cave, presented high relative abundances of the genus wb1-P19, followed by *Crossiella* and *Nitrospira*, CARD-FISH experiments showed that *Actinomycetota* forms the core of yellow biofilms. In fact, fragmentation of substrate mycelium into rod-shaped elements (Labeda, 2001) is evident in Fig. 6 and this point to the main role of *Crossiella* in shaping the biofilm and its spatial arrangement (Fig. 6h). Based on microscopic and taxonomic results, we propose an evolutionary model where mostly rod-shaped *Actinomycetota* forms the filaments with appendages that intertwine and give rise to the branches, which originates the yellow biofilms of Pindal Cave. These fiber-like appendages may be essential for colony formation and adhesion (Fig. S1) and nutrient uptake by retaining water droplets and suspended material on their surface (El Othmany et al., 2021). Then, these biofilms would evolve in yellow complex biofilms composed by other bacteria (Fig. S1). Although to the naked eye the biofilms present different morphologies, the results confirm that the yellow biofilms in Pindal Cave have stable microstructures (Figs. 5 and 6).

The gammaproteobacterial genus wb1-P19 (*Nitrosococcaceae*) was one of the most abundant groups in many caves (Holmes et al., 2001; Schabereiter-Gurtner et al., 2002a, 2002b; Zhu et al., 2019; Frazier, 2020; Jurado et al., 2020; Liñán et al., 2021; Reboleira et al., 2022). According

to Holmes et al. (2001) the unnamed genus wb1-P19 clustered phylogenetically with sulfur and/or nitrite-oxidizing autotrophic bacteria, but information on their metabolism is scarce. Likewise, Martin-Pozas et al. (2022a) suggested a syntrophic relationship between *Crossiella* and wb1-P19 and linked both genera to CO_2 uptake in moonmilk deposits in Pindal Cave.

The network co-occurrence analysis (Fig. S2) revealed similar results in Pindal yellow biofilms suggesting an association of *Crossiella*, wb1-P19 and *Nitrospira* in this cave. The genus wb1-P19 was previously found in the yellow biofilms from two Appalachian limestone caves (Frazier, 2020). Similarly, the genus *Nitrosococcus*, which belongs to the family *Nitrosococcaceae* (recorded as *Chromatiaceae* in the NCBI Taxonomy database), were previously found in yellow biofilms from lava caves (Spilde et al., 2016). *Crossiella* (*Pseudonocardiaceae*) is a genus relatively abundant in caves, soils, plant rhizospheres, and building stones, although rarely isolated (Engelbrecht et al., 2021; Gonzalez-Pimentel et al., 2021; Guerra et al., 2022; Martin-Pozas et al., 2022a; Martin-Pozas et al., 2023). *Nitrospira* is a genus that comprises ammonium-oxidizing bacteria and is

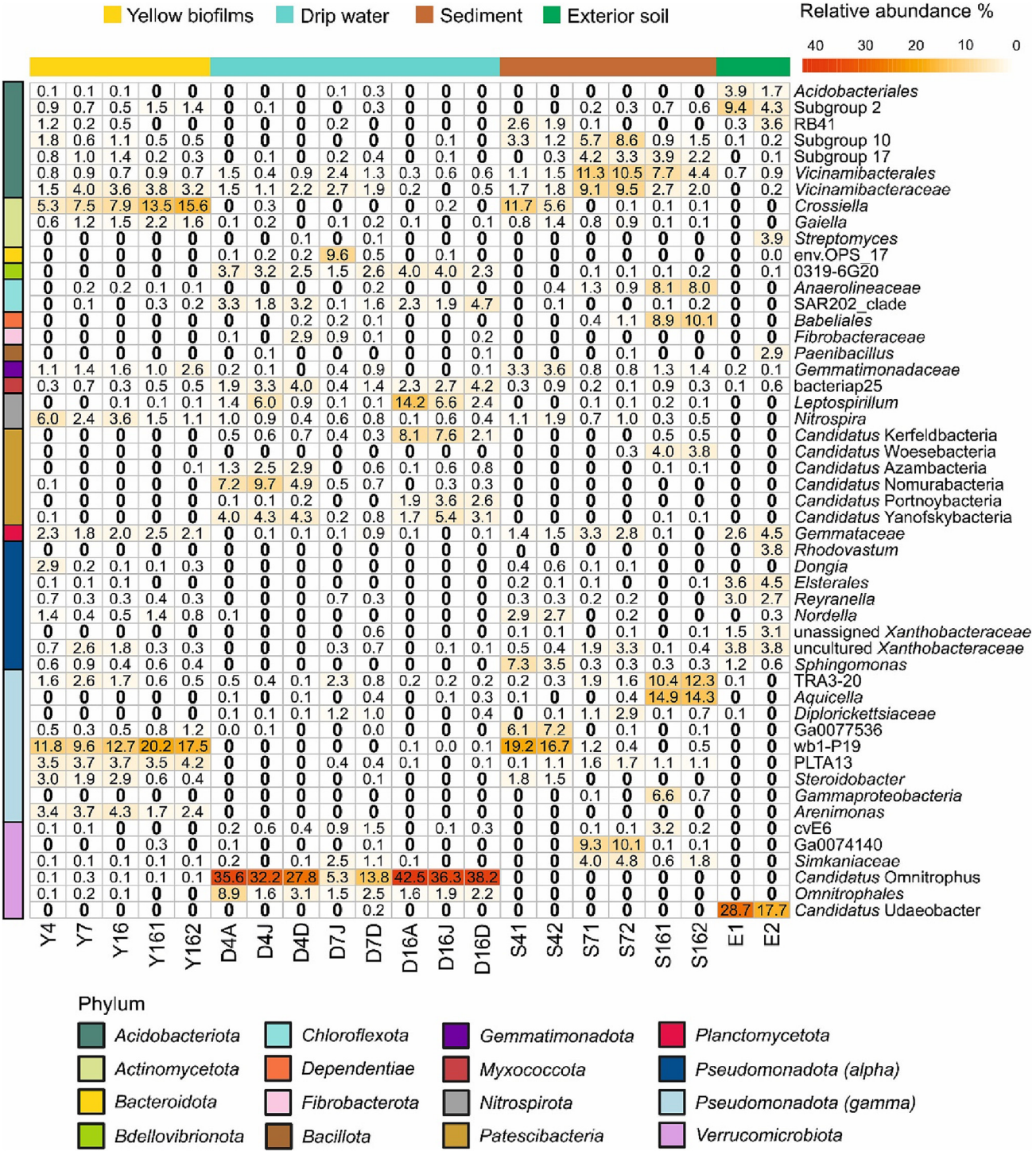

Fig. 9. Heatmap highlighting the relative abundances of the most abundant reads. 0 means relative abundance lower than 0.05 %. Colors from white to red indicate represent the relative abundance. Taxa are displayed on the Y axis, samples on the X axis. The legend located at the top indicates the type of sample, while the legend to the right indicates the phylum to which each sequence corresponds.

relatively frequent in Spanish caves (Jurado et al., 2020; Martin-Pozas et al., 2020; Gonzalez-Pimentel et al., 2021), and have a widespread presence in other caves (Chen et al., 2009; Pasic et al., 2010; Northup et al., 2011; Wu et al., 2015; De Mandal et al., 2017; Oliveira et al., 2017).

Other less abundant, but characteristic members of yellow biofilms from Pindal Cave, was *Arenimonas*. Members of the genus *Arenimonas* were previously recorded in caves (Spilde et al., 2016; Wiseschart et al., 2019), and were isolated from mines, soils and aquatic environments (Chen et al., 2012; Liu et al., 2018; Han et al., 2020). In fact, previous studies on yellow biofilms from limestone and lava caves related the presence of members of the order *Xanthomonadales*, which included *Arenimonas* (Portillo et al., 2008; Porca et al., 2012; Spilde et al., 2016; Gonzalez-Pimentel et al., 2018; He et al., 2020).

A few authors reported that the color of yellow biofilms could be due to the abundance of *Proteobacteria*, and likely corresponded to the presence of members of the orders *Chromatiales* and *Xanthomonadales*, known by their production of carotenoids which could be responsible for the yellow coloration (Portillo et al., 2008).

Identified genera and family with relative abundances >1 % (Fig. 5) were *Vicinamibacteraceae*, *Crossiella*, *Nitrospira*, *Arenimonas*, *Steroidobacter*, *Xanthobacteraceae*, *Dongia*, *Gemmataceae*, *Gemmatimonadaceae* and *Nordella*. Most of these bacteria have yellow colors. In fact, the family *Vicinamibacteraceae* (subdivision 6 of *Acidobacteria*) only contains two genera described so far, *Vicinamibacter* and *Luteitalea*, both showing yellow color (Huber and Overmann, 2018).

The color of the mycelium in *Crossiella cryophila* (*Pseudonocardiaceae*) was yellowish to light yellow (Labeda, 2001), as well as for *Nitrospira* (Watson et al., 1986), *Arenimonas* (Kwon et al., 2007; Makk et al., 2015), and *Steroidobacter* (Huang et al., 2019). Finally, *Xanthobacteraceae* members have yellow color due to the presence of the carotenoid zeoxanthin dirhamnoside (Oren, 2014).

Porca et al. (2012) in a previous study compared phylotype distribution in yellow biofilms from geographically distinct limestone caves (Spain, Czech Republic and Slovenia) and concluded that *Pseudonocardiaceae* (*Actinomycetota*), *Gammaproteobacteria* (*Pseudomonadota*) and *Nitrospirota* constitute the core of the microbial communities, similarly to that observed in Pindal yellow biofilms. Different authors found similar data in other yellow biofilms from lava and limestone caves (Pasic et al., 2010; Riquelme et al., 2015b; Lavoie et al., 2017).

Surprisingly, Gonzalez-Pimentel et al. (2018) described a morphologically and taxonomically different type of yellow biofilms in a lava cave, which could indicate that there exists more than one type of yellow cave biofilms. The yellow biofilms described by Gonzalez-Pimentel et al. (2018) presented high relative abundances of the order *Chromatiales*, followed by *Euzebyales*. Other studies showed similar results (Riquelme et al., 2015a; Spilde et al., 2016; Frazier, 2020). Remarkably, in one of the Appalachian caves, described by Frazier (2020), the yellow biofilms showed high relative abundances of wb1-P19, *Crossiella*, and *Nitrospira*, and 22 groups were coincident between the yellow biofilms of Pindal and RN5 cave. However, the genus *Euzebya*, abundant in RN5 cave was not present in Pindal, and *Arenimonas*, abundant in Pindal was not found in RN5 cave. These results reinforce the theory that there is more than one type of yellow biofilm, with distinct morphologies and bacterial compositions: one type dominated by the family *Pseudonocardiaceae*, similar to Pindal biofilms, and another type dominated by the order *Euzebyales*, similar to the biofilms described by Gonzalez-Pimentel et al. (2018). Together all the results indicate that the classification by color is not enough to describe yellow biofilms.

4.2. Specific bacterial groups depends on the substrata (exterior soil, rock, sediment, drip water)

The exterior soils overlaying Pindal Cave showed substantially different bacterial communities from subsurface communities as previously reported by Lavoie et al. (2017) for other caves. In our study, surface soil samples do not show greater diversity indices than cave samples. In fact, we observed a higher diversity in yellow biofilms (Fig. 7a). In general, the diversity indices of yellow biofilms from Pindal Cave were higher than those found in other limestone and lava caves (Pasic et al., 2010; Lavoie et al., 2017; Riquelme et al., 2015b; Gonzalez-Pimentel et al., 2018). Overlap in ASVs between surface and cave communities were only 12 % and NMDS showed differences between exterior soil and cave communities suggesting that most of exterior soil microorganisms do not enter the cave. Some abundant bacterial groups in exterior soils such as *Candidatus* Udaeobacter, *Acidobacteriales*, the subdivision 2 of *Acidobacteriota*, *Elsterales*, *Reyranella*, unassigned *Xanthobacteraceae*, and *Streptomyces* (Schlatter and Kinkel, 2014; Arias-Giraldo et al., 2021; Pessi et al., 2022; Rodriguez et al., 2022; M.-C. Shen et al., 2022) showed low relative abundances in subsurface samples. The adverse cave environmental conditions could explain this decreased of relative abundances of some soil microorganisms, as suggested by the Microbial Conveyor Belt (Mestre and Höfer, 2021). *Candidatus* Udaeobacter is an abundant and ubiquitous soil verrucomicrobial clade that shows preference for acid pH (Brewer et al., 2016; Willms et al., 2021; Rodriguez et al., 2022). The subdivision 2 of *Acidobacteriota*, together with uncultured *Acidobacteriales*, were abundant in soils (Jones et al., 2009; Ivanova et al., 2020) and positively correlated with organic carbon content and negatively with pH (Liu et al., 2016). The moderately basic pH of sediments in Pindal Cave could explain the low relative abundance of these taxa.

In this study, yellow biofilms, sediments and exterior soils presented higher percentages of *Acidobacteriota* than waters. This phylum has been described in nearly all ecosystems and represents a significant fraction of soil microbial community. The subdivisions 10 and 17 of *Acidobacteriota* showed higher abundances in sediments than in the yellow biofilms while the family *Vicinamibacteraceae* showed similar relative abundances in all underground samples. Although both taxa have been described in caves around the world and in different types of substrata such as vermiculations, moonmilks and mineral deposits, previous studies did not reported these differences (Zimmermann et al., 2005; Miller et al., 2020; Addesso et al., 2021; Gonzalez-Pimentel et al., 2021; Martin-Pozas et al., 2022a; J. Shen et al., 2022).

Overlap in ASVs between yellow biofilms and cave sediments was only 6 %, while NMDS and taxonomic results suggest that yellow biofilm communities were similar to sediments, especially to materials found in the site 4 (Fig. 6b and c). As mentioned before, gravity coarse-grained deposits prevail at site 4, constituted of a mixture of small breakdown blocks of bedrock and speleothems, while sediments from sites 7 and 16 were associated to suspended sediment (mud) transported by the river. The genera wb1-P19, *Crossiella*, *Nitrospira*, *Arenimonas* and *Steroidobacter* were the most abundant groups in yellow biofilms but also appeared with abundances over 1 % in sediments of site 4. These genera generally appear in cave walls and colored biofilms, which suggest a preference by rock and speleothems substrata (Riquelme et al., 2015b; Lavoie et al., 2017; Zhu et al., 2019; Frazier, 2020; Jurado et al., 2020; Gonzalez-Pimentel et al., 2021; Liñán et al., 2021). Non-metric dimensional scaling (NMDS) and Venn diagram in Fig. 7 show a separation of the drip water from the yellow biofilms, sediments and exterior soil samples. The phylum *Bdellovibrionota*, the phylum *Myxococcota*, SAR202_clade of the phylum *Chloroflexota*, the genus *Leptospirillum* (*Nitrospirota*), most members of the phylum *Patescibacteria* and the order *Omnitrophales* showed higher relative abundances in drip waters while its representation is very poor in the rest of the samples of this study (Figs. 8 and 9). The SAR202_clade includes abundant bacteria in the deep ocean but it was also recorded in aquifers (Kirs et al., 2020) and soils (Geng et al., 2020; Betterman et al., 2021). The class bacteriap25 was also recorded in aquatic environments (Pedron et al., 2022; Rubin-Blum et al., 2022) and soils (Betterman et al., 2021; Darriaut et al., 2023) and cave manganese patinas (Bernardini et al., 2021). The genus *Leptospirillum* comprises acidophilic ferrous iron and manganese oxidizer bacteria and are involved in acid mine drainage (Denef and Banfield, 2012; Urbieta et al., 2012). The high relative abundance of *Leptospirillum* in Pindal drip waters is surprising since some samples shows very low content of manganese and iron. *Omnitrophales* and

Patescibacteria, among other groups, were included in the so-called rare cave biosphere (Hershey and Barton, 2018), or microbial dark matter (Wiegand et al., 2018). According to the results of Pindal Cave, these two phyla are mainly retrieved from groundwater environments (Griebler and Lueders, 2009; Herrmann et al., 2019; Wegner et al., 2019; Tian et al., 2020). Herrmann et al. (2019) reported that *Patescibacteria* were preferentially mobilized from soils and flourish under oligotrophic conditions in groundwaters, reaching high relative abundances (17 to 79 %). Therefore, Pindal drip waters communities have a structure similar to those groundwaters of different geographical regions and diverse from those yellow biofilms and sediments.

Biogeochemical features of dripping waters reflect different paths and water/rock interaction rates occurring along different water flow paths (Fairchild et al., 2000). The ratios of alkali metals (Mg/Ca, Ba/Ca, and Sr/Ca) of drip water and speleothems are a potential proxy for present and past hydrological conditions, respectively (Stoll et al., 2012). For instance, during periods of low flow, prior calcite precipitation (PCP) could preferentially remove Ca^{2+} from dripwaters, elevating these ratios (Fairchild et al., 2006). The concentrations of Mg, Sr, and Ba may be also enriched during low flow periods due to greater contribution of seepage water which features longer water-rock and water-soil contact times (Wong et al., 2011). Calculating the dissimilarity between the bacterial community composition of drip water samples revealed separation mostly strongly based on the partial pressure of carbon dioxide (pCO_2), pH, ATP, NO_3^-, NaCl, and sulfate content (Fig. 7d). The drip water from site 16 also showed NO_3^- anomalous values (Table S4), which are related to the farm activity in the soil over the cave (Martin-Pozas et al., 2022b). In this area, the drip water composition reflects an intensive water-rock interaction: it presents high Ca^{2+} and HCO_3^-, and Mg/Ca molar ratio that even may indicate prior calcite precipitation. Contrarily, the drip water from site 7 presents a lower water-rock interaction, which is reflected in the Ca^{2+} and HCO_3^- concentration and pCO_2 in equilibrium. The drip waters in site 7 shows different microbiology features and a higher average ATP with higher percentages of *Bdellovibrionota* X0319-6G20, *Sphingobacteriales* and *Bacteroidota* env.OPS 17. Under these conditions, we found a lower percentage of *Leptospirillum* and *Candidatus Omnitrophus*, which can be indicative taxa of low water-rock interaction (Fig. S3). Finally, D4 contains the highest marine ion concentrations which is related with high percentages of *Candidatus* Nomurabacteria.

4.3. Bioclimatic factors affecting Pindal Cave bacterial communities

The spatiotemporal features of cave air temperature enable a direct assessment of the influence of meteorological changes (daily and seasonal) and climatic trends of the local external atmosphere on the indoor-outdoor thermal gradient. This gradient plays a key role in the aerodynamic processes determining the ventilation or stagnation of air masses, as well as the sudden temporal and spatial variations of temperature that would potentially trigger vapor condensation processes in the cave-rock and sediments surfaces. The vapor content of a saturated air mass decreases as the temperature suddenly decreases due to condensation under isobaric settings, forming water droplets attached to airborne particles or to the colder and exposed rock surfaces to the main air currents.

In the case of Pindal Cave, the greatest proliferation of yellow biofilms seems to be associated with areas where there is strong condensation due to daily or seasonal temperature variations that cause air currents that meet a cooler surface at the entrance, on rock protrusions, walls, or narrow areas. Inner cave morphology also plays a key role in the present spatial pattern of biofilms, which mainly colonize the surfaces located in front of the main trajectories of air currents and, consequently, with a high frequency of naked eye observed condensation droplets. Therefore, it may be inferred the spatial relationship between the probable and confirmed areas with condensations and the distribution and ecological features of the yellow biofilms. In this regard, the aerial hyphae of *Actinomycetota* colonizing cave-rock surfaces and sediments might act as vapor condensation nuclei (Fig. 5c) and, in turn, water controls their metabolic activity and the microbe-mineral interactions. Some other studies identified excessive humidity as the key environmental factor that triggers microbial breakout events. He et al. (2021) suggested that humidity and the North orientation of the Maijishan Grottoes were the main cause of the microbe outbreak in its ancient wall paintings. These factors enhanced the water content in the wall surfaces due to continuous condensation, particularly during raining seasons and poor ventilation of the cave (He et al., 2022). Aiming to assess this spatial relationship, a regular grid of points estimated for air temperature (expressed as annual mean) was transformed using the statistical tool gradient operator (GO, hereafter), in the same way as Fernandez-Cortes et al. (2006) used it for spatiotemporal analysis of cave air temperature as an environmental management tool. This grid calculation generates a new grid of the steepest slopes of air temperature (i.e. the magnitude of its spatial gradient in terms of variation of air temperature per meter) at any point on the cave map, which is then compared with the distribution of the yellow bacteria colonies. Indeed, GO is close to zero for those cave zones where air temperature barely varies in any direction and, conversely, it reaches maximum values as the spatial correlation is greater. These last zones are characterized by sudden spatial and temporal variations of air temperature that likely favor the vapor condensation on the colder surfaces or, even, in the form of hydro-aerosols.

The spatial distribution of the gradient operator for air temperature throughout a hydrological year reveals new information about the zonation of microclimate stability at Pindal Cave (Fig. 10). The gradient operator of air temperature highlights transition zones where temperature shows a greater spatial variation (i.e., a larger OG) and, conversely, the more stable areas are associated with stagnant air (i.e., lower OG).

The largest mean gradient operators were calculated for the cave zones between sites 1 and 4, which are the sites closest to the entrance and where the spatial correlation of air temperature is highest. As mentioned before, in Pindal Cave yellow biofilms communities were similar to sediments in site 4. These sediments are completely different from the others, because they are composed of the remains of speleothems as the result of the dissolution of cave walls by condensation water. This process is particularly efficient near cave entrances where the thermal gradient is high. Based on thermal gradient data, the yellow biofilm formation could be linked to condensation-corrosion processes, which can explain the presence of similar bacterial communities in the sediments from site 4.

Away from these zones, air temperature is more spatially stable and records lower GO values, particularly in zones between sites 7 and 11 (Fig. 10), and GO reaches the minimum values in the inner-most sector of the cave (site 17 and hereafter). There are other inner zones with medium to high gradient operator values, which also separate sections of galleries with greater thermal stability. These intermediate zones connect consecutive compartmentalized areas of the cave, separated by giant flowstones that act as barriers to the movement of cave air masses (Figs. 1 and 2; cave sectors between sites 13 and 16).

By comparing the distribution of the yellow bacteria colonies, in the high-density colonization area near the cave entrance prevails intense daily fluctuations of air (>0.15 °C/day; Fig. 2), and the highest GO values (Fig. 10). These thermal instabilities cause a greater condensation of water, mainly in the area around the site 4, where the cave section is considerably reduced and the east-facing rock surfaces partially block against the external airflow. In this sense, it is very noticeable the high frequency of condensation pulses in this cave sector registered during the summer (Fig. 4).

Field observations confirm the abundance of condensation droplets and yellow biofilms on the cave walls in those areas of the cave with high OG values for temperature (e.g., site 4), but also in the area furthest from the main entrance (site 17 and hereafter). Here, OG reaches minimum values but frequent condensation pulses are registered due to the likely inflow of external and warmer air following the riverbed, particularly during summer (Fig. 4). Likewise, other inner zones with high OG values for temperature would reveal a hidden condensation, i.e. not perceptible to the naked eye, as the tiny droplets are quickly absorbed by biofilms or become part of the interstitial water in the surface pore system of the non-colonized

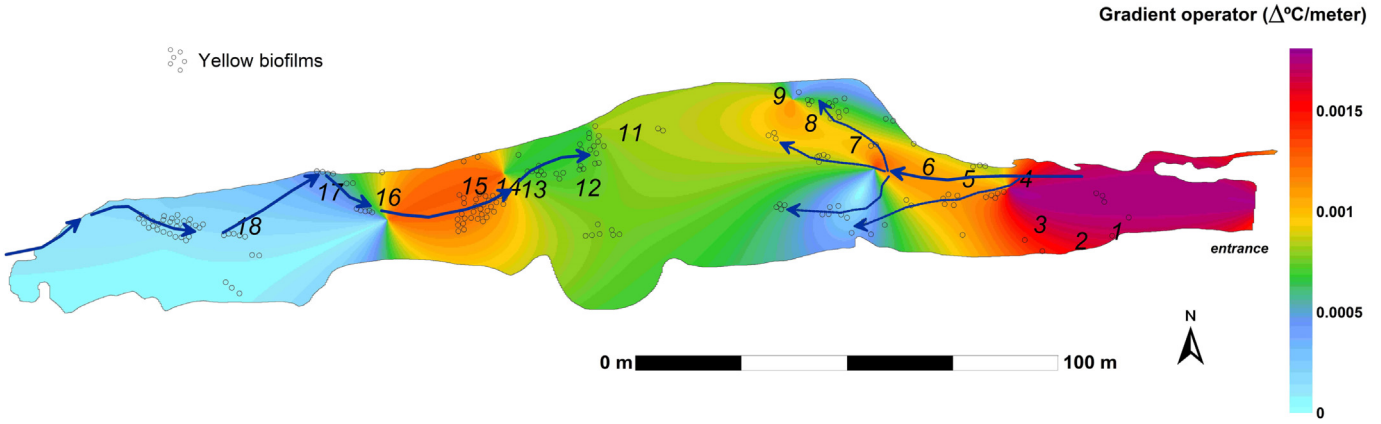

Fig. 10. Spatial distribution of the gradient operator (GO) for the mean air temperature at Pindal Cave. Monitoring period: October 2021–September 2022. The distribution of the yellow biofilms is drawn for comparison. Numbers indicate the lighting sites located along the tourist path. Blue arrows mark the trajectory of the airflow; this preferentially follows the intermittent riverbed in the inner zones of the cave.

rock or cave sediments. On the contrary, there is hardly any colonization of yellow biofilms in intermediate zones (between sites 9 and 11), where moderate temporal fluctuation of air temperature (<0.15 °C/day; Fig. 2) and low GO values are registered. In this cave zone, the desiccation cracks in the soil sediments are often observable, which are indicative of reduced wetting as the condensation water supply is reduced and evaporation prevails.

4.4. Origin of core members of yellow biofilms in Pindal Cave

The top-three core members of yellow biofilms from Pindal Cave were wb1-P19, *Crossiella* and *Nitrospira*. In our study, none of these reads appears in the exterior soil samples. However, these genera have been described in exterior soils (Daims et al., 2001; Lavoie et al., 2017; Adeyemo and Onilude, 2018; Goodfellow et al., 2018; Krauze et al., 2021; Guerra et al., 2022). Porca et al. (2012) suggested that the core of yellow biofilms might be true cave dwellers that come into the cave through water infiltration from the overlaying rock. Some abundant reads in yellow biofilms, for example *Nitrospira*, TRA3-20, *Vicinamibacterales*, *Gemmataceae*, and *Gemmatimonadaceae*, also appeared with low percentages in almost all drip water samples, indicating that probably come into the cave through water drips. To our knowledge, no previous drip water environmental DNA metabarcoding studies supported the entry of these bacteria through the water infiltration (Marques et al., 2019). However, other abundant reads in yellow biofilms such as *Crossiella*, wb1-P19, *Arenimonas*, *Steroidobacter*, PLTA13 do not appear or hardly appear represented in the drip water samples. The community composition in the cave biofilms differs markedly from that of the seepage water samples. On the contrary, the bacterial communities of the biofilms show significant similarities with those of the sediments, especially with the sediment samples from zone 4 (ecotone) where the most abundant species in the biofilms also appear as the majority in the sediments (Fig. 9). These results suggest that sediments can act as reservoirs, which can subsequently grow and form biofilms under favorable environmental and substrate conditions, primarily on speleothems and rocks with rough surfaces located in preferential condensation zones. The subsequent movement of particles from sediments through air currents, anthropic activities, etc., may serve as an important vector, although not the only one, for the proliferation and dispersion of biofilms towards areas with less favorable environmental conditions.

To summarized, based on environmental and taxonomic analyses we hypothesize that the colonization of bacteria occurring in cave yellow biofilms arose through two different ways: water infiltration and air currents that transport bacteria to cooler rock surfaces. Aerobiology studies based on independent culture techniques in cave systems are very scarce (Zhu et al., 2019). These authors reported that *Actinomycetota* dominated the sediment and rock samples and were absent in air samples. The authors identified *Xanthomonadaceae* as indicator genus of air samples, supporting our airborne colonization hypothesis but did not discuss about the origin of *Crossiella* or *Nitrosococcaceae* wb1-P19. Therefore, nowadays remains a key knowledge gap on the source of cave microbial communities but the set of analytical and observational data suggest that the bioclimatic conditions are the main factor affecting the origin and development of this type of biofilm.

5. Concluding remarks

To conclude, comparison between yellow biofilms from Pindal Cave and yellow biofilms described in previous studies by other authors indicates that color classification is not enough to describe cave biofilms, and other approaches such as ultrastructure, morphology and taxonomic composition are necessary.

The microbial communities from Pindal yellow biofilms showed a different composition from that of the exterior soils and drip waters. In fact, only *Nitrospira* and other less abundant genera showed low relative abundances in all drip waters while other abundant genera in yellow biofilms (wb1-P19 and *Crossiella*) were missing or present in negligible relative abundances in drip waters and exterior soils. Therefore, the most abundant bacteria in the yellow biofilms could enter the cave by multiple other routes not only the infiltration water. In this study, the environmental results pointed that abundance of yellow biofilms is related to condensation events. The results indicate that sediments play a crucial role as reservoirs and sources of bacteria, which can then colonize and develop into biofilms under favorable environmental and substrate conditions. The transportation of sediment particles through air currents, anthropic activities, and other means emerges as a key mechanism for the proliferation and dispersion of biofilms into areas with less conducive environmental conditions. Particularly, speleothems and rough-surfaced rocks located in condensation-prone areas serve as preferred sites for biofilm formation. These findings shed light on the dynamics and potential spread of biofilms, highlighting the importance of sediment contributions and their subsequent impact on ecosystem processes and microbial colonization patterns.

We propose a model for the formation of this type of yellow biofilm, based on microscopy and environmental results. Free cells of *Crossiella* (a widely distributed bacterium in soils) from surface and underground sediments attach to the cave surfaces and form the first filaments that will subsequently form the branches of the biofilm. In the following stages, other bacteria were associated to *Crossiella* filaments to evolve into complex biofilms.

This point to the need of performing complete metagenomics studies including air, water, sediments, biofilms and exterior soils in order combined to FISH experiments and environmental monitoring to understand the dynamic of cave microbial communities and to decipher the origin of cave

biofilms. These studies could be helpful to understand the environmental conditions and the nutritional requirements to microorganisms that usually dwell in cave environments to design conservation strategies for cave art. The findings derived from this microbiological and environmental study have direct implications for decision-making and sustainable cave management. Although there is not a single cave conservation strategy, the first corrective measure that is needed to adopt would consist of the implantation of metal grids in the busiest areas of the cave. This would be an effective and low-impact measure to reduce the resuspension of particles caused by visitors during tourist visits and research activities.

Supplementary data to this article can be found online at https://doi.org/10.1016/j.scitotenv.2023.165218.

Funding

This research was supported by the Spanish Ministry of Science and Innovation through project PID2019-110603RB-I00 and the collaboration of PID2020-114978GB-I00 project, MCIN/AEI/FEDER, UE/10.13039/501100011033. This is a contribution from CSIC Interdisciplinary Thematic Platform Open Heritage: Research and Society (PTI-PAIS).

CRediT authorship contribution statement

Conceptualization, SSM, AFC, SC, TMP; investigation, TMP, JCC, SSM, AFC, SC, DB, ED; writing—original draft preparation, TMP, SSM, AFC, SC, JCC, CSJ; writing—review and editing, TMP, SSM, AFC, CSJ. All authors contributed to the interpretation of the data and provided significant input to the final manuscript. All authors have read and agreed to the published version of the manuscript.

Data availability statement

The 16S rRNA gene sequences and accompanying metadata have been deposited in the Sequence Read Archive (SRA) of NCBI under the project number PRJNA885499.

Declaration of competing interest

The authors declare that they have no known competing financial interests or personal relationships that could have appeared to influence the work reported in this paper.

Acknowledgments

The authors would like to thank the Electron Microscopy facility of CBMSO (UAM-CSIC) and the Analysis Service by NON-Destructive Techniques of MNCN (CSIC), especially Milagros Guerra Rodriguez for their assistance in TEM sample preparation and Marta Furió Vega for their photographic assistance. The authors would like to thank Dr. Bernhard Fuchs, Dr. Monike Oggerin de Orube and Andreas Ellrott of Max-Planck-Institut fuer Marine Mikrobiologie for their assistance with CARD-FISH and Airyscan confocal microscopy. We thank Maria Gonzalez-Pumariega Solís (Consejería de Cultura del Principado de Asturias) for her technical assistance during fieldwork and her valuable advice as an expert on the Pindal Cave.

References

Addesso, R., Gonzalez-Pimentel, J.L., D'Angeli, I.M., De Waele, J., Saiz-Jimenez, C., Jurado, V., Miller, A.Z., Cubero, B., Vigliotta, G., Baldantoni, D., 2021. Microbial community characterizing vermiculations from karst caves and its role in their formation. Microb. Ecol. 81, 884–896. https://doi.org/10.1007/s00248-020-01623-5.

Adeyemo, O., Onilude, A., 2018. Antimicrobial potential of a rare actinomycete isolated from soil: *Crossiella* sp.-EK18. J. Adv. Microbiol. 11, 1–15. https://doi.org/10.9734/JAMB/2018/41989.

Alonso, L., Pommier, T., Simon, L., Maucourt, F., Doré, J., Dubost, A., Trân Van, V., Minard, G., Valiente Moro, V., Douady, C.J., Moënne-Loccoz, Y., 2023. Microbiome analysis in Lascaux Cave in relation to black stain alterations of rock surfaces and collembola. Environ. Microbiol. Rep. 15 (2), 80–91. https://doi.org/10.1111/1758-2229.13133 in press.

Arias-Giraldo, L.F., Guzmán, G., Montes-Borrego, M., Gramaje, D., Gómez, J.A., Landa, B.B., 2021. Going beyond soil conservation with the use of cover crops in Mediterranean sloping olive orchards. Agronomy 11, 1387. https://doi.org/10.3390/agronomy11071387.

Bastian, F., Jurado, V., Novakova, A., Alabouvette, C., Saiz-Jimenez, C., 2010. The microbiology of the Lascaux Cave. Microbiology 156, 644–652. https://doi.org/10.1099/mic.0.036160-0.

Bernardini, S., Bellatreccia, F., Columbu, A., Vaccarelli, I., Pellegrini, M., Jurado, V., Del Gallo, M., Saiz-Jimenez, C., Sodo, A., Millo, C., Jovane, L., De Waele, J., 2021. Morpho-mineralogical and bio-geochemical description of cave manganese stromatolite-like patinas (Grotta del Cervo, Central Italy) and hints on their paleohydrological-driven genesis. Front. Earth Sci. 9, 642667. https://doi.org/10.3389/feart.2021.642667.

Betterman, A., Zethof, J.H.T., Babin, D., Cammeraat, E.L.H., Solé-Benet, A., Lázaro, R., Luna, L., Nesme, J., Sørensen, S.J., Kalbitz, K., Smalla, K., Vogel, C., 2021. Importance of microbial communities at the root-soil interface for extracellular polymeric substances and soil aggregation in semiarid grasslands. Soil Biol. Biochem. 159, 108301. https://doi.org/10.1016/j.soilbio.2021.108301.

Blott, S.J., Pye, K., 2001. GRADISTAT: a grain size distribution and statistics package for the analysis of unconsolidated sediments. Earth Surf. Process. Landf. 26, 1237–1248. https://doi.org/10.1002/ESP.261.

Bolyen, E., Rideout, J.R., Dillon, M.R., Bokulich, N.A., Abnet, C., Al-Ghalith, G.A., et al., 2019. Reproducible, interactive, scalable, and extensible microbiome data science using QUIIME 2. Nat. Biotechnol. 37, 852–857. https://doi.org/10.1038/s41587-019-0209-9.

Brewer, T.E., Handley, K.M., Carini, P., Gilbert, J.A., Fierer, N., 2016. Genome reduction in an abundant and ubiquitous soil bacterium '*Candidatus* Udaeobacter copiosus'. Nat. Microbiol. 2, 16198. https://doi.org/10.1038/nmicrobiol.2016.198.

Callahan, B.J., McMurdie, P.J., Rosen, M.J., Han, A.W., Johnson, A.J.A., Holmes, S.P., 2016. DADA2: high-resolution sample inference from Illumina amplicon data. Nat. Methods 13, 581–583. https://doi.org/10.1101/024034.

Cañaveras, J.C., Sanchez-Moral, S., Soler, V., Saiz-Jimenez, C., 2001. Microorganisms and microbially induced fabrics in cave walls. Geomicrobiol J. 18, 223–240. https://doi.org/10.1080/01490450152467769.

Chen, Y., Wu, L., Boden, R., Hillebrand, A., Kumaresan, D., Moussard, H., Baciu, M., Lu, Y., Murrell, J.C., 2009. Life without light: microbial diversity and evidence of sulfur- and ammonium-based chemolithotrophy in Movile Cave. ISME J. 3, 1093–1104. https://doi.org/10.1038/ismej.2009.57.

Chen, F., Shi, Z., Wang, G., 2012. *Arenimonas metalli* sp. nov., isolated from an iron mine. Int. J. Syst. Evol. Microbiol. 62, 1744–1749. https://doi.org/10.1099/ijs.o.034132-0.

Cuezva, S., Sanchez-Moral, S., Saiz-Jimenez, C., Cañaveras, J.C., 2009. Microbial communities and associated mineral fabrics in Altamira Cave, Spain. Int. J. Speleol. 38, 83–92. https://doi.org/10.5038/1827-806X.38.1.9.

Cuezva, S., Fernandez-Cortes, A., Porca, E., Pašić, L., Jurado, V., Hernandez- Marine, M., Ortiz-Serrano, P., Hermosin, B., Cañaveras, J.C., Sanchez-Moral, S., Saiz-Jimenez, C., 2012. The biogeochemical role of *Actinobacteria* in Altamira Cave, Spain. FEMS Microbiol. Ecol. 81, 281–290. https://doi.org/10.1111/j.1574- 6941.2012.01391.x.

Daims, H., Nielsen, J.L., Nielsen, P.H., Schleifer, K.H., Wagner, M., 2001. In situ characterization of Nitrospira-like nitrite-oxidizing bacteria active in wastewater treatment plants. Appl. Environ. Microbiol. 67, 5273–5284. https://doi.org/10.1128/AEM.67.11.5273-5284.2001.

Darriaut, R., Tran, J., Martins, G., Ollat, N., Masneuf-Pomarède, I., Lauvergeat, V., 2023. In grapevine decline, microbiomes are affected differently in symptomatic and asymptomatic soils. Appl. Soil Ecol. 183, 104767. https://doi.org/10.1016/j.apsoil.2022.104767.

De Mandal, S., Chatterjee, R., Kumar, N.S., 2017. Dominant bacterial phyla in caves and their predicted functional roles in C and N cycle. BMC Microbiol. 17, 90. https://doi.org/10.1186/s12866-017-1002-x.

Denef, V.J., Banfield, J.F., 2012. In situ evolutionary rate measurements show ecological success of recently emerged bacterial hybrids. Science 336, 462–466. https://doi.org/10.1126/science.1218389.

El Othmany, R., Zahir, H., Ellouali, M., Latrache, H., 2021. Current understanding on adhesion and biofilm development in *Actinobacteria*. Int. J. Microbiol. 2021, 6637438. https://doi.org/10.1155/2021/6637438.

Engelbrecht, G., Claassens, S., Mienie, C.M.S., Fourie, H., 2021. Screening of rhizosphere bacteria and nematode populations associated with soybean roots in the Mpumalanga Highveld of South Africa. Microorganisms 9, 1813. https://doi.org/10.3390/microorganisms9091813.

Fairchild, I.J., Borsato, A., Tooth, A.F., Frisia, S., Hawkesworth, C.J., Huang, Y.M., McDermott, F., Spiro, B., 2000. Controls on trace element (Sr-Mg) compositions of carbonate cave waters: implications for speleothem climatic records. Chem. Geol. 166 (3–4), 255–269. https://doi.org/10.1016/S0009-2541(99)00216-8.

Fairchild, I.J., Tuckwell, G.W., Baker, A., Tooth, A.F., 2006. Modelling of dripwater hydrology and hydrogeochemistry in a weakly karstified aquifer (Bath, UK): implications for climate change studies. J. Hydrol. 321 (1–4), 213–231. https://doi.org/10.1016/j.jhydrol.2005.08.002.

Fernandez-Cortes, A., Calaforra, J.M., Sanchez-Martos, F., 2006. Spatiotemporal analysis of air conditions as a tool for the environmental management of a show cave (Cueva del Agua, Spain). Atmos. Environ. 40, 7378–7394. https://doi.org/10.1016/j.atmosenv.2006.06.045.

Fernandez-Cortes, A., Cuezva, S., Sanchez-Moral, S., Porca, E., Jurado, V., Saiz-Jimenez, C., 2011. Detection of human-induced environmental disturbances in a show cave. Environ. Sci. Pollut. Res. 18, 1037–1045. https://doi.org/10.1007/s11356-011-0513-5.

Frazier, V.E., 2020. Carbon Metabolism in Cave Subaerial Biofilms. University of Tennessee. https://trace.tennessee.edu/utk_gradthes/5867 (Master's Thesis).

Geng, S., Cao, W., Yuan, J., Wang, Y., Guo, Y., Ding, A., Zhu, Y., Dou, J., 2020. Microbial diversity and co-occurrence patterns in deep soils contaminated by polycyclic aromatic hydrocarbons (PAHs). Ecotoxicol. Environ. Saf. 203, 110931. https://doi.org/10.1016/j.ecoenv.2020.110931.

Gonzalez-Pimentel, J.L., Martin-Pozas, T., Jurado, V., Miller, A.Z., Caldeira, A.T., Fernandez-Lorenzo, O., Sanchez-Moral, S., Saiz-Jimenez, C., 2021. Prokaryotic communities from a lava tube cave in La Palma Island (Spain) are involved in the biogeochemical cycle of major elements. PeerJ 9, e11386. https://doi.org/10.7717/peerj.11386.

Gonzalez-Pimentel, J.L., Miller, A.Z., Jurado, V., Laiz, L., Pereira, M.F.C., Saiz-Jimenez, C., 2018. Yellow colored mats from lava tube of La Palma (Canary Islands, Spain) are dominated by metabolically active Actinobacteria. Sci. Rep. 8, 1944. https://doi.org/10.1038/s41598-018-20393-2.

González-Pumariega Solís, M., 2011. La cueva de El Pindal, 1911-2011. Estudio de su arte rupestre cien años después de Les Cavernes de la Région Cantabrique. Ménsula Ediciones, Pola de Siero.

Goodfellow, M., Nouioui, I., Sanderson, R., Xie, F., Bull, A.T., 2018. Rare taxa and dark microbial matter: novel bioactive actinobacteria abound in Atacama Desert soils. Anton. Leeuw. 111, 1315–1332. https://doi.org/10.1007/s10482-018-1088-7.

Griebler, C., Lueders, T., 2009. Microbial biodiversity in groundwater ecosystems. Freshw. Biol. 54, 649–677. https://doi.org/10.1111/j.1365-2427.2008.02013.x.

Guerra, V.A., Beule, L., Mackowiak, C.L., Dubeux Jr, J.C.B., Blount, A.R.S., Wang, X.-B., Rowland, D.L., Liao, H.-L., 2022. Soil bacterial community response to rhizoma peanut incorporation into Florida pastures. J. Environ. Qual. 2022 (51), 55–65. https://doi.org/10.1002/jeq2.20307.

Han, D.M., Chun, B.H., Kim, H.M., Khan, S.A., Jeon, C.O., 2020. *Arenimonas terrae* sp. nov., isolated from orchard soil. Int. J. Syst. Evol. Microbiol. 70, 537–542. https://doi.org/10.1099/ijsem.0.003785.

Hathaway, J.J.M., Garcia, M.G., Balasch, M., Spilde, M.N., Stone, F.D., Dapkevicius, M.L.N.E., Amorim, I.R., Gabriel, R., Borges, P.A.V., Northup, D.E., 2014. Comparison of bacterial diversity in Azorean and Hawai'ian lava cave microbial mats. Geomicrobiol J. 31, 205–220. https://doi.org/10.1080/01490451.2013.777491.

He, Y.-W., Cao, X.-Q., Poplawsky, A.R., 2020. Chemical structure, biological roles, biosynthesis and regulation of the yellow xanthomonadin pigments in the phytopathogenic genus *Xanthomonas*. Mol. Plant-Microbe Interact. 33, 705–714. https://doi.org/10.1094/MPMI-11-19-0326-CR.

He, D.P., Wu, F.S., Ma, W.X., Zhang, Y., Gu, J.D., Duan, Y.L., Xu, R.H., Feng, H.Y., Wang, W.F., Li, S.W., 2021. Insights into the bacterial and fungal communities and microbiome that causes a microbe outbreak on ancient wall paintings in the Maijishan Grottoes. Int. Biodeterior. Biodegrad. 163, 105250. https://doi.org/10.1016/j.ibiod.2021.105250.

He, D., Wu, F., Ma, W., Gu, J.D., Xu, R., Hu, J., Yue, Y., Ma, Q., Wang, W., 2022. Assessment of cleaning techniques and its effectiveness for controlling biodeterioration fungi on wall paintings of Maijishan Grottoes. Int. Biodeterior. Biodegrad. 171, 105406. https://doi.org/10.1016/j.ibiod.2022.105406.

Herlemann, D.P., Labrenz, M., Jürgens, K., Bertilsson, S., Waniek, J.J., Andersson, A.F., 2011. Transitions in bacterial communities along the 2000 km salinity gradient of the Baltic Sea. ISME J. 5, 1571–1579. https://doi.org/10.1038/ismej.2011.41.

Herrmann, M., Wegner, C.-E., Taubert, M., Geesink, P., Lehmann, K., Yan, L., Lehmann, R., Totsche, K.U., Küsel, K., 2019. Predominance of *Ca.* Patescibacteria in groundwater is caused by their preferential mobilization from soils and flourishing under oligotrophic conditions. Front. Microbiol. 10, 1407. https://doi.org/10.3389/fmicb.2019.01407.

Hershey, O.S., Barton, H.A., 2018. Microbial diversity in caves. In: Moldovan, O., Kovác, L., Halse, S. (Eds.), Cave Ecology. Springer, New York, pp. 69–90 https://doi.org/10.1007/978-3-319-98852-8.

Holmes, A.J., Tujula, N.A., Holley, M., Contos, A., James, J.M., Rogers, P., Gillings, M.R., 2001. Phylogenetic structure of unusual aquatic microbial formations in Nullarbor caves, Australia. Environ. Microbiol. 3, 256–264. https://doi.org/10.1046/j.1462-2920.2001.00187.x.

Hoshino, T., Yilmaz, L.S., Noguera, D.R., Daims, H., Wagner, M., 2008. Quantification of target molecules needed to detect microorganisms by fluorescence in situ hybridization (FISH) and catalyzed reporter deposition-FISH. Appl. Environ. Microbiol. 74, 5068. https://doi.org/10.1128/AEM.00208-08.

Huang, J.-W., Hu, S.-L., Cheng, X.-K., Chen, D., Kong, X.-K., Jiang, J.D., 2019. *Steroidobacter soli* sp. nov., isolated from farmland soil. Int. J. Syst. Evol. Microbiol. 69, 3443–3447.

Huber, K.J., Overmann, J., 2018. *Vicinamibacteraceae* fam. nov., the first described family within the subdivision 6 *Acidobacteria*. Int. J. Syst. Evol. Microbiol. 68, 2331–2334. https://doi.org/10.1099/ijsem.0.002841.

Ishii, K., Mußmann, M., MacGregor, B.J., Amann, R., 2004. An improved fluorescence in situ hybridization protocol for the identification of bacteria and archaea in marine sediments. FEMS Microbiol. Ecol. 50, 203–213. https://doi.org/10.1016/J.FEMSEC.2004.06.015.

Ivanova, A.A., Zhelezova, A.D., Chernov, T.I., Dedysh, S.N., 2020. Linking ecology and systematics of acidobacteria: distinct habitat preferences of the *Acidobacteriia* and *Blastocatellia* in tundra soils. PLoS One 15, e0230157. https://doi.org/10.1371/journal.pone.0230157.

Jimenez-Sanchez, M., Bischoff, J.L., Stoll, H., Aranburu, A., 2006. A geochronological approach for cave evolution in the Cantabrian Coast (Pindal Cave, NW Spain). Z. Geomorph. N. F., Suppl. 147, 129–141.

Jones, R.T., Robeson, M.S., Lauber, C.L., Hamady, M., Knight, R., Fierer, N., 2009. A comprehensive survey of soil acidobacterial diversity using pyrosequencing and clone library analyses. ISME J. 3, 442–453. https://doi.org/10.1038/ismej.2008.127.

Jurado, V., Gonzalez-Pimentel, J.L., Miller, A.Z., Hermosin, B., D'Angeli, I.M., Tognini, P., De Waele, J., Saiz-Jimenez, C., 2020. Microbial communities in vermiculation deposits from an Alpine cave. Front. Earth Sci. 8, 586248. https://doi.org/10.3389/feart.2020.586248.

Kim, J.-S., Kim, D.-S., Lee, K.C., Kim, Y.-H., Ahn, U.-S., Lee, M.-K., Lee, J.-S., 2019. Yellow-colored mats in Jeju Island lava tubes. J. Kor. Appl. Sci. Technol. 36, 1338–1348. https://doi.org/10.12925/jkocs.2019.36.4.1338.

Kirs, M., Kisand, V., Nelson, C.E., Dudoit, T., Moravcik, P.S., 2020. Distinct bacterial communities in tropical island aquifers. PLoS One 15, e0232265. https://doi.org/10.1371/journal.pone.0232265.

Krauze, P., Wagner, D., Spinola, D.N., Kühn, P., 2021. Influence of prokaryotic microorganisms on initial soil formation along a glacier forefield on King George Island, maritime Antarctica. Sci. Rep. 11, 13135. https://doi.org/10.1038/s41598-021-92205-z.

Kwon, S.-W., Kim, B.-Y., Weon, H.-Y., Baek, Y.-K., Go, S.-J., 2007. *Arenimonas donghaensis* gen. nov., sp. nov., isolated from seashore sand. Int. J. Syst. Evol. Microbiol. 57, 954–958. https://doi.org/10.1099/ijs.0.64457-0.

Labeda, D.P., 2001. *Crossiella* gen. nov., a new genus related to *Streptoalloteichus*. Int. J. Syst. Evol. Microbiol. 51, 575–579.

Laiz, L., Groth, I., Gonzalez, I., Saiz-Jimenez, C., 1999. Microbiological study of the dripping waters in Altamira cave (Santillana del Mar, Spain). J. Microbiol. Methods 36, 129–138. https://doi.org/10.1016/S0167-7012(99)00018-4.

Lavoie, K.H., Winter, A.S., Read, K.J.H., Hughes, E.M., Spilde, M.N., Northup, D.E., 2017. Comparison of bacterial communities from lava cave microbial mats to overlying surface soils from Lava Beds National Monument, USA. PLoS One 12, e0169339. https://doi.org/10.1371/journal.pone.0169339.

Liñán, C., Benavente, J., del Rosal, Y., Vadillo, I., Ojeda, L., Carrasco, F., 2021. Condensation water in heritage touristic caves: isotopic and hydrochemical data and a new approach for its quantification through image analysis. Hydrol. Process. 35, e14083. https://doi.org/10.1002/hyp.14083.

Liu, J., Sui, Y., Yu, Z., Yao, Q., Shi, Y., Chu, H., Jin, J., Liu, X., Wang, G., 2016. Diversity and distribution patterns of acidobacterial communities in the black soil zone of northeast China. Soil Biol. Biochem. 95, 212–222. https://doi.org/10.1016/j.soilbio.2015.12.021.

Liu, J.-l., Yao, J., Wang, F., Ni, W., Liu, X.-y., Sunahara, G., Duran, R., Jordan, G., Hudson-Edwards, K.A., Alakangas, L., Solevic-Knudsen, T., Zhu, X.-z., Zhang, Y.-y., Li, Z.-f., 2018. China's most typical nonferrous organic-metal facilities own specific microbial communities. Sci. Rep. 8, 12570. https://doi.org/10.1038/s41598-018-30519-1.

Ma, W., Wu, F., He, D., Li, J., Zhang, Q., Yang, X., Gu, J.-D., Wang, W., Feng, H., 2023. The biodeterioration outbreak in Dunhuang Mogao Grottoes analyzed for the microbial communities and the occurrence time by C-14 dating. Int. Biodeterior. Biodegradation 178, 105533. https://doi.org/10.1016/j.ibiod.2022.105533.

Makk, J., Homonnay, Z.G., Kéki, Z., Nemes-Barnás, K., Márialigeti, K., Schumann, P., Tóth, E.M., 2015. *Arenimonas subflava* sp. nov., isolated from a drinking water network, and emended description of the genus *Arenimonas*. Int. J. Syst. Evol. Microbiol. 65, 1915–1921. https://doi.org/10.1099/ijs.0.000201.

Marques, E.L.S., Silva, G.S., Dias, J.C.T., Gross, E., Costa, M.S., Rezende, R.P., 2019. Cave drip water-related samples as a natural environment for aromatic hydrocarbon-degrading bacteria. Microorganisms 7, 33. https://doi.org/10.3390/microorganisms7020033.

Martin-Pozas, T., Sanchez-Moral, S., Cuezva, S., Jurado, V., Saiz-Jimenez, C., Perez-Lopez, R., Carrey, R., Otero, N., Giesemann, A., Well, R., Calaforra, J.M., Fernandez-Cortes, A., 2020. Biologically mediated release of endogenous N_2O and NO_2 gases in a hydrothermal, hypoxic subterranean environment. Sci. Total Environ. 747, 141218. https://doi.org/10.1016/j.scitotenv.2020.141218.

Martin-Pozas, T., Cuezva, S., Fernandez-Cortes, A., Cañaveras, J.C., Benavente, D., Jurado, V., Saiz-Jimenez, C., Janssens, I., Seijas, N., Sanchez-Moral, S., 2022a. Role of subterranean microbiota in the carbon cycle and greenhouse gas dynamics. Sci. Total Environ. 831, 154921. https://doi.org/10.1016/j.scitotenv.2022.154921.

Martin-Pozas, T., Cuezva Robleño, S., Fernández Cortés, Á., Gónzalez-Pumariega Solís, M., Cañaveras, J.C., Benavente, D., Goy Goy, J.L., Elez Villar, J., Saiz Jiménez, C., Zazo Cardeña, C., Sánchez-Moral, S., 2022b. Impacto de un evento de inundación en la comunidad bacteriana de un ecosistema subterráneo somero (Cueva del Pindal, Asturias). In: Calaforra, J.M., Durán, J.J. (Eds.), Minas y Cuevas: Patrimonio Geológico y Turístico. Asociación de Cuevas Turísticas Españolas, Madrid. ISBN: 978-84-123288-2-0, pp. 261–274.

Martin-Pozas, T., Gonzalez-Pimentel, J.L., Jurado, V., Laiz, L., Cañaveras, J.C., Fernandez-Cortes, A., Cuezva, S., Sanchez-Moral, S., Saiz-Jimenez, C., 2023. *Crossiella*, a rare *Actinomycetota* genus, abundant in the environment. Appl. Biosci. 2, 194–210. https://doi.org/10.3390/applbiosci2020014.

McMurdie, P.J., Holmes, S., 2013. Phyloseq: an R package for reproducible interactive analysis and graphics of microbiome census data. PLoS One 8, e61217. https://doi.org/10.1371/journal.pone.0061217.

Mestre, M., Höfer, J., 2021. The microbial conveyor belt: connecting the globe through dispersion and dormancy. Trends Microbiol. 29, 482–492. https://doi.org/10.1016/j.tim.2020.10.007.

Miller, A.Z., García-Sánchez, A.M., Coutinho, M.L., Pereira, M.F.C., Gázquez, F., Calaforra, J.M., Forti, P., Martínez-Frías, J., Toulkeridis, T., Caldeira, A.T., Saiz-Jimenez, C., 2020. Colored microbial coatings in show caves from the Galapagos Islands (Ecuador): first microbiological approach. Coatings 10, 1134. https://doi.org/10.3390/coatings10111134.

Mulec, J., Oarga-Mulec, A., Tomazin, R., Matos, T., 2015. Characterization and fluorescence of yellow biofilms in karst caves, southwest Slovenia. Int. J. Speleol. 44, 107–114. https://doi.org/10.5038/1827-806X.44.2.1.

Mulec, J., Oarga-Mulec, A., Sturm, S., Tomazin, R., Matos, T., 2017. Spacio-temporal distribution and tourist impact on airborne bacteria in a cave (Škocjan Caves, Slovenia). Diversity 9, 28. https://doi.org/10.3390/d9030028.

Northup, D.E., Melim, L.A., Spilde, M.N., Hathaway, J.J.M., Garcia, M.G., Moya, M., Stone, F.D., Boston, P.J., Dapkevicius, M.L.N.E., Riquelme, C., 2011. Lava cave microbial communities within mats and secondary mineral deposits: implications for life detection on other planets. Astrobiology 11, 601–618. https://doi.org/10.1089/ast.2010.0562.

Oliveira, C., Gunderman, L., Coles, C.A., Lochmann, J., Parks, M., Ballard, E., Glazko, G., Rahmatallah, Y., Tackett, A.J., Thomas, D.J., 2017. 16S rRNA gene-based metagenomic analysis of Ozark Cave bacteria. Diversity 9, 31. https://doi.org/10.3390/d9030031.

Oren, A., 2014. The family *Xanthobacteraceae*. In: Rosenberg, E., et al. (Eds.), The Prokaryotes – *Alphaproteobacteria* and *Betaproteobacteria*. Springer, Berlin, pp. 709–726.

Oren, A., Garrity, G.M., 2021. Valid publication of the names of forty-two phyla of prokaryotes. Int. J. Syst. Evol. Microbiol. 71 (10), 005056. https://doi.org/10.1099/ijsem.0.005056.. 34694987.

Parkhurst, D.L., Appelo, C.A.J., 2013. Description of input and examples for PHREEQC version 3—a computer program for speciation, batch-reaction, one-dimensional transport, and inverse geochemical calculations. US Geological Survey Techniques and Methods Book 6, Chapter A43, 497 p http://pubs.usgs.gov/tm/06/a43.

Pasic, L., Kovce, B., Sket, B., Herzog-Velikonja, B., 2010. Diversity of microbial communities colonizing the walls of a Karstic cave in Slovenia. FEMS Microbiol. Ecol. 71, 50–60. https://doi.org/10.1111/j.1574-6941.2009.00789.x.

Pedron, R., Esposito, A., Cozza, W., Paolazzi, M., Cristofolini, M., Segata, N., Jousson, O., 2022. Microbiome characterization of alpine water springs for human consumption reveals site- and usage-specific microbial signatures. Front. Microbiol. 13, 946460. https://doi.org/10.3389/fmicb.2022.946460.

Pernthaler, A., Pernthaler, J., 2007. Fluorescence in situ hybridization for the identification of environmental microbes. Methods Mol. Biol. 353, 153–164. https://doi.org/10.1385/1-59745-229-7:153.

Pessi, I.S., Viitamäki, S., Virkkala, A.-M., Eronen-Rasimus, E., Delmont, T.O., Marushchak, M.E., Luoto, M., Hultman, J., 2022. In-depth characterization of denitrifier communities across different soil ecosystems in the tundra. Environ. Microbiome 17, 30. https://doi.org/10.1186/s40793-022-00424-2.

Porca, E., Jurado, V., Zgur-Bertok, D., Saiz-Jimenez, C., Pasic, L., 2012. Comparative analysis of yellow microbial communities growing on the walls of geographically distinct caves indicates a common core of microorganisms involved in their formation. FEMS Microbiol. Ecol. 81, 255–266. https://doi.org/10.1111/j.1574-6941-2012.01383.x.

Portillo, M.C., Gonzalez, J.M., Saiz-Jimenez, C., 2008. Metabolically active microbial communities of yellow and grey colonizations on the walls of Altamira Cave, Spain. J. Appl. Microbiol. 104, 681–691. https://doi.org/10.1111/j.1365-2672.2007.03594.x.

Priest, T., Fuchs, B., Amann, R., Reich, M., 2021. Diversity and biomass dynamics of unicellular marine fungi during a spring phytoplankton bloom. Environ. Microbiol. 23, 448–463. https://doi.org/10.1111/1462-2920.15331.

Quast, C., Pruesse, E., Yilmaz, P., Gerken, J., Schweer, T., Yarza, P., Peplies, J., Glöckner, F.O., 2013. The SILVA ribosomal RNA gene database project: improved data processing and web-based tools. Nucleic Acids Res. 41, D590–D596. https://doi.org/10.1093/nar/gks1219.

Reboleira, A.S., Bodawatta, K.H., Ravn, N.M.R., Lauritzen, S.-E., Skoglund, R.O., Poulsen, M., Michelsen, A., Jonsson, K.A., 2022. Nutrient-limited subarctic caves harbor more diverse and complex bacterial communities than their surface soil. Environ. Microbiome 17, 41. https://doi.org/10.1186/s40793-022-00435-z.

Riquelme, C., Hathaway, J.J.M., Dapkevicius, M.L.E., Miller, A.Z., Kooser, A., Northup, D.E., Jurado, V., Fernandez, O., Saiz-Jimenez, C., Cheeptham, N., 2015a. Actinobacterial diversity in volcanic caves and associated geomicrobiological interactions. Front. Microbiol. 6, 1342. https://doi.org/10.3389/fmicb.2015.01342.

Riquelme, C., Rigal, F., Hathaway, J.J.M., Northup, D.E., Spilde, M.N., Borges, P.A.V., Gabriel, R., Amorin, I.R., Dapkevicius, M.L.N.E., 2015b. Cave microbial community composition in oceanic islands: disentangling the effect of different colored mats in diversity patterns of Azorean lava caves. FEMS Microbiol. Ecol. 91, fiv141. https://doi.org/10.1093/femsec/fiv141.

Rodriguez, V., Moskwa, L.-M., Oses, R., Kühn, P., Riveras-Muñoz, N., Seguel, O., Scholten, T., Wagner, D., 2022. Impact of climate and slope aspects on the composition of soil bacterial communities involved in pedogenetic processes along the Chilean Coastal Cordillera. Microorganisms 10, 847. https://doi.org/10.3390/microorganisms10050847.

Rubin-Blum, M., Sisma-Ventura, G., Yudkovski, Y., Belkin, N., Kanari, M., Herut, B., Rahav, E., 2022. Diversity, activity, and abundance of benthic microbes in the Southeastern Mediterranean Sea. FEMS Microbiol. Ecol. 98, fiac009. https://doi.org/10.1093/femsec/fiac009.

Saiz-Jimenez, C., Cuezva, S., Jurado, V., Fernandez-Cortes, A., Porca, E., Benavente, D., Cañaveras, J.C., Sanchez-Moral, S., 2011. Paleolithic art in peril: policy and science collide at Altamira Cave. Science 334, 2. https://doi.org/10.1126/science.1206788.

Saiz-Jimenez, C., Miller, A.Z., Martin-Sanchez, P.M., Hernandez-Marine, M., 2012. Uncovering the origin of the black stains in Lascaux Cave in France. Environ. Microbiol. 14, 3220–3231. https://doi.org/10.1111/1462-2920.12008.

Schabereiter-Gurtner, C., Saiz-Jimenez, C., Piñar, G., Lubitz, W., Rolleke, S., 2002a. Altamira cave paleolithic paintings harbour partly unknown bacterial communities. FEMS Microbiol. Lett. 211, 7–11. https://doi.org/10.1016/S0378-1097(02)00668-7.

Schabereiter-Gurtner, C., Saiz-Jimenez, C., Piñar, G., Lubitz, W., Rölleke, S., 2002b. Phylogenetic 16S rRNA analysis reveals the presence of complex and partly unknown bacterial communities in Tito Bustillo cave, Spain, and on its Palaeolithic paintings. Environ. Microbiol. 4, 392–400. https://doi.org/10.1046/j.1462-2920.2002.00303.x.

Schlatter, D.C., Kinkel, L.L., 2014. Global biogeography of *Streptomyces* antibiotic inhibition, resistance, and resource use. FEMS Microbiol. Ecol. 88, 386–397. https://doi.org/10.1111/1574-6941.12307.

Selensky, M.J., Masterson, A.L., Blank, J.G., Lee, S.C., Osburn, M.R., 2021. Stable carbon isotope depletions in lipid biomarkers suggest subsurface carbon fixation in lava caves. J. Geophys. Res. Biogeosci. 126, e2021JG006430. https://doi.org/10.1029/2021JG006430.

Shen, J., Smith, A.C., Barnett, M.J., Morgan, A., Wynn, P.M., 2022a. Distinct microbial communities in the soils, waters, and speleothems of a hyperalkaline cave system. J. Geophys. Res. Biogeosci. 127, e2022JG006866. https://doi.org/10.1029/2022JG006866.

Shen, M.-C., Zhang, Y.-Z., Bo, G.-D., Yang, B., Wang, P., Ding, Z.-Y., Wang, Z.-B., Yang, J.-M., Zhang, P., Yuan, X.-L., 2022b. Microbial responses to the reduction of chemical fertilizers in the rhizosphere soil of flue- cured tobacco. Front. Bioeng. Biotechnol. 9, 812316. https://doi.org/10.3389/fbioe.2021.812316.

Spilde, M.N., Northup, D.E., Caimi, N.A., Boston, P.J., Stone, F.D., Smith, S., 2016. Microbial mat communities in Hawaiian lava caves. International Symposium on Vulcanospeleology 2016 . https://www.cavepics.com/IVS17/SPILDE.pdf.

Sterflinger, K., Little, B., Pinar, G., Pinzari, F., de los Rios, A., Gu, J.-D., 2018. Future directions and challenges in biodeterioration research on historic materials and cultural properties. Int. Biodeterior. Biodegradation 129, 10–12. https://doi.org/10.1016/j.ibiod.2017.12.007.

Stoll, H.M., Müller, W., Prieto, M., 2012. I-STAL, a model for interpretation of Mg/Ca, Sr/Ca and Ba/Ca variations in speleothems and its forward and inverse application on seasonal to millennial scales. Geochem. Geophys. Geosyst. 13, Q09004. https://doi.org/10.1029/2012GC004183.

Tian, R., Ning, D., He, Z., Zhang, P., Spencer, S.J., Gao, S., Shi, W., Wu, L., Zhang, Y., Yang, Y., Adams, B.G., Rocha, A.M., Detienne, B.L., Lowe, K.A., Joyner, D.C., Klingeman, D.M., Arkin, A.P., Fields, M.W., Hazen, T.C., Stahl, D.A., Alm, E.J., Zhou, J., 2020. Small and mighty: adaptation of superphylum *Patescibacteria* to groundwater environment drives their genome simplicity. Microbiome 8, 1–15. https://doi.org/10.1186/s40168-020-00825-w.

Urbieta, M.S., Gonzalez Toril, E., Aguilera, A., Giaveno, M.A., Donati, E., 2012. First prokaryotic biodiversity assessment using molecular techniques of an acidic river in Neuquen, Argentina. Microb. Ecol. 64, 91–104. https://doi.org/10.1007/s00248-011-9997-2.

Urzì, C., De Leo, F., Bruno, L., Albertano, P., 2010. Microbial diversity in Paleolithic caves: a study case on the phototrophic biofilms of the Cave of Bats (Zuheros, Spain). Microb. Ecol. 60, 116–129. https://doi.org/10.1007/s00248-010-9710-x.

Walker, P.H., Hutka, J., 1971. Use of the Coulter Counter (Model B) for particle-size analysis of soils. CSIRO Div. Soils Tech. Pap. 1. ISBN: 9780643008670, pp. 1–39.

Watson, S.W., Bock, E., Valois, F.W., Waterbury, J.B., Schlosser, U., 1986. *Nitrospira marina* gen. nov. sp. nov.: a chemolithotrophic nitrite-oxidizing bacterium. Arch. Microbiol. 144, 1–7.

Wegner, C.E., Gaspar, M., Geesink, P., Herrmann, P., Marz, M., Küsel, K., 2019. Biogeochemical regimes in shallow aquifers reflect the metabolic coupling of the elements nitrogen, sulfur, and carbon. Appl. Environ. Microbiol. 85, e02346-18. https://doi.org/10.1128/AEM.02346-18.

White, T.J., Bruns, T., Lee, S., Taylor, J., 1990. Amplification and direct sequencing of fungal ribosomal RNA genes for phylogenetics. In: Innis, M.A., Gelfand, D.H., Sninsky, J.J., White, T.J. (Eds.), PCR Protocols: A Guide to Methods and Applications. Academic Press, London, pp. 315–322.

Wiegand, S., Jogler, M., Jogler, C., 2018. On the maverick Planctomycetes. FEMS Microbiol. Rev. 42, 739–760. https://doi.org/10.1093/femsre/fuy029.

Willms, I.M., Bolz, S.H., Yuan, J., Kraff, L., Schneider, D., Schöning, I., Schrumpf, M., Nacke, H., 2021. The ubiquitous soil verrucomicrobial clade '*Candidatus* Udaeobacter' shows preferences for acidic pH. Environ. Microbiol. Rep. 13, 878–883. https://doi.org/10.1111/1758-2229.13006.

Wiseschart, A., Mhuantong, W., Tangphatsornruang, S., Chantasingh, D., Pootanakit, K., 2019. Shotgun metagenomic sequencing from Manao-Pee cave, Thailand, reveals insight into the microbial community structure and its metabolic potential. BMC Microbiol. 19, 144. https://doi.org/10.1186/s12866-019-1521-8.

Wong, C.I., Banner, J.L., Musgrove, M., 2011. Seasonal dripwater Mg/Ca and Sr/Ca variations driven by cave ventilation: implications for and modeling of speleothem paleoclimate records. Geochim. Cosmochim. Acta 75 (12), 3514–3529. https://doi.org/10.1016/j.gca.2011.03.025.

Wu, Y., Tan, L., Liu, W., Wang, B., Wang, J., Cai, Y., Lin, X., 2015. Profiling bacterial diversity in a limestone cave of the western Loess Plateau of China. Front. Microbiol. 6, 244. https://doi.org/10.3389/fmicb.2015.00244.

Zerboni, A., Villa, F., Wu, Y.-L., Solomon, T., Trentini, A., Rizzi, A., Cappitelli, F., Gallinaro, M., 2022. The sustainability of rock art: preservation and research. Sustainability 14, 6305. https://doi.org/10.3390/su14106305.

Zhang, G., Gong, C., Gu, J., Katayama, Y., Someya, T., Gu, J.-D., 2019. Biochemical reactions and mechanisms involved in the biodeterioration of stone world cultural heritage under the tropical climate conditions. Int. Biodeterior. Biodegradation 143, 104723. https://doi.org/10.1016/j.ibiod.2019.104723.

Zhu, H.-Z., Zhang, Z.-F., Zhou, N., Jiang, C.-Y., Wang, B.-J., Cai, L., Liu, S.-J., 2019. Diversity, distribution and co-occurrence patterns of bacterial communities in a karst cave system. Front. Microbiol. 10, 1726. https://doi.org/10.3389/fmicb.2019.01726.

Zimmermann, J., Gonzalez, J.M., Saiz-Jimenez, C., Ludwig, W., 2005. Detection and phylogenetic relationships of highly diverse uncultured acidobacterial community on paleolithic paintings in Altamira Cave using 23S rRNA sequence analyses. Geomicrobiol J. 22, 379–388. https://doi.org/10.1080/01490450500248986.